

# Federated Learning for Privacy-Preserving Medical AI

**Tin Hoang**

*Master of Science in Artificial Intelligence*

from the

University of Surrey



UNIVERSITY OF  
**SURREY**

*School of Computer Science and Electrical and Electronic Engineering*

Faculty of Engineering and Physical Sciences

University of Surrey

Guildford, Surrey, GU2 7XH, UK

September 2025

Supervised by: Prof. Gustavo Carneiro

©Tin Hoang 2025

## **DECLARATION OF ORIGINALITY**

I confirm that the project dissertation I am submitting is entirely my own work and that any material used from other sources has been clearly identified and properly acknowledged and referenced. In submitting this final version of my report to the JISC anti-plagiarism software resource, I confirm that my work does not contravene the university regulations on plagiarism as described in the Student Handbook. In so doing I also acknowledge that I may be held to account for any particular instances of uncited work detected by the JISC anti-plagiarism software, or as may be found by the project examiner or project organiser. I also understand that if an allegation of plagiarism is upheld via an Academic Misconduct Hearing, then I may forfeit any credit for this module or a more severe penalty may be agreed.

MSc Dissertation Title: Federated Learning for Privacy-Preserving Medical AI

Author Name: Tin Huu Hoang

Author Signature:

Date: 02/09/2025

Supervisor's name: Prof. Gustavo Carneiro

**WORD COUNT**

Number of Pages: 91

Number of Words: 15940

## ABSTRACT

Federated learning offers a transformative approach to collaborative medical artificial intelligence by enabling institutions to jointly develop robust diagnostic models while maintaining strict patient privacy and data sovereignty. This dissertation investigates privacy-preserving federated learning for Alzheimer’s disease classification using three-dimensional MRI data from the Alzheimer’s Disease Neuroimaging Initiative (ADNI). Existing methodologies often suffer from unrealistic data partitioning, inadequate privacy guarantees, and insufficient benchmarking, limiting their practical deployment in healthcare. To address these gaps, this research proposes a novel site-aware data partitioning strategy that preserves institutional boundaries, reflecting real-world multi-institutional collaborations and data heterogeneity. Furthermore, an Adaptive Local Differential Privacy (ALDP) mechanism is introduced, dynamically adjusting privacy parameters based on training progression and parameter characteristics, thereby significantly improving the privacy-utility trade-off over traditional fixed-noise approaches. Systematic empirical evaluation across multiple client federations and privacy budgets demonstrated that advanced federated optimisation algorithms, particularly FedProx, could equal or surpass centralised training performance while ensuring rigorous privacy protection. Notably, ALDP achieved up to 80.4% accuracy in a two-client configuration, surpassing fixed-noise Local DP by 5–7 percentage points and demonstrating substantially greater training stability. The comprehensive ablation studies and benchmarking establish quantitative standards for privacy-preserving collaborative medical AI, providing practical guidelines for real-world deployment. This work thereby advances the state-of-the-art in federated learning for medical imaging, establishing both methodological foundations and empirical evidence necessary for future privacy-compliant AI adoption in healthcare. The source code for this dissertation is available at: [github.com/Tin-Hoang/fl-adni-classification](https://github.com/Tin-Hoang/fl-adni-classification)

1

---

<sup>1</sup>Experiments tracked at: <https://wandb.ai/tin-hoang/fl-adni-classification>

## CONTENTS

<b>Declaration of Originality</b>	<b>ii</b>
<b>Word Count</b>	<b>iii</b>
<b>Abstract</b>	<b>iv</b>
<b>List of figures</b>	<b>ix</b>
<b>List of tables</b>	<b>xi</b>
<b>1 Introduction</b>	<b>1</b>
1.1 Background and Context . . . . .	1
1.2 Objectives . . . . .	2
1.3 Achievements . . . . .	3
1.4 Overview of Dissertation . . . . .	4
<b>2 Background Theory and Literature Review</b>	<b>7</b>
2.1 Medical AI and the Challenge of Data Fragmentation . . . . .	7
2.1.1 Neuroimaging and Alzheimer’s Disease Classification . . . . .	7
2.2 Privacy and Regulatory Challenges in Centralised Medical AI . . . . .	8
2.2.1 Technical and Legal Barriers to Data Sharing . . . . .	8
2.2.2 Security Risks and Data Breach Implications . . . . .	10
2.3 Theoretical Foundations of Federated Learning . . . . .	10
2.3.1 Core Components and Communication Protocols . . . . .	10
2.3.2 Federated Averaging (FedAvg) . . . . .	10
2.3.3 Federated Proximal (FedProx) . . . . .	12
2.4 Privacy-Preserving Technologies for Federated Learning . . . . .	12
2.4.1 Local DP: Differential Privacy in Federated Learning . . . . .	12
2.4.2 SecAgg+: Secure Aggregation Protocols . . . . .	14

2.5	Federated Learning in Healthcare: Current State and Limitations . . . . .	15
2.5.1	Medical Imaging Applications . . . . .	15
2.5.2	Neuroimaging and Alzheimer’s Disease Detection . . . . .	15
2.6	Research Gaps and Opportunities . . . . .	16
2.6.1	Site-Aware Data Partitioning for Realistic Federated Scenarios . . . . .	16
2.6.2	Differential Privacy Exploration for Neuroimaging Applications . . . . .	17
2.6.3	Adaptive Privacy Mechanism Development . . . . .	17
2.6.4	Algorithmic Benchmarking of Advanced Strategies . . . . .	18
2.7	Positioning of Current Research . . . . .	18
2.8	Chapter Summary . . . . .	19
<b>3</b>	<b>Methodology</b>	<b>21</b>
3.1	Site-Aware Data Partitioning: Realistic Federated Learning Simulation . . . . .	21
3.1.1	Motivation and Problem Formulation . . . . .	21
3.1.2	Site-Aware Distribution Algorithm . . . . .	22
3.1.3	Methodological Advantages . . . . .	23
3.2	Adaptive Local Differential Privacy: A Novel Privacy Mechanism . . . . .	23
3.2.1	Motivation: Limitations of Fixed-Noise Differential Privacy . . . . .	24
3.2.2	ALDP Algorithm . . . . .	25
3.2.3	Temporal Privacy Budget Adaptation . . . . .	27
3.2.4	Per-Tensor Variance-Aware Noise Scaling . . . . .	28
3.3	Summary . . . . .	28
<b>4</b>	<b>Implementation and Integration</b>	<b>30</b>
4.1	FL Framework Selection . . . . .	30
4.1.1	Selection Criteria and Justification . . . . .	30
4.1.2	Flower Framework Advantages for Medical Imaging Research . . . . .	31
4.2	Medical Imaging Framework Integration . . . . .	33
4.3	System Architecture Overview . . . . .	33

4.3.1	Integration and Coordination Principles . . . . .	34
4.3.2	Federated Learning Core . . . . .	35
4.3.3	Medical Imaging Pipeline . . . . .	35
4.3.4	Local and Distributed Deployment Infrastructure . . . . .	36
4.3.5	Experiment Tracking and Monitoring . . . . .	37
4.4	Summary . . . . .	37
<b>5</b>	<b>Experimental Setup</b>	<b>39</b>
5.1	Dataset Acquisition and Preprocessing . . . . .	39
5.1.1	ADNI Data Collection . . . . .	39
5.1.2	Image Preprocessing Pipeline . . . . .	39
5.1.3	Data Quality Assurance and Duplicate Removal . . . . .	41
5.2	Data Filtering and Label Conversion . . . . .	41
5.2.1	Initial Dataset Composition . . . . .	41
5.2.2	Label Conversion . . . . .	41
5.2.3	Final Dataset Statistics . . . . .	41
5.3	Federated Data Splitting: Multi-Client Scenarios . . . . .	43
5.3.1	On-the-fly Data Augmentation Strategy . . . . .	44
5.4	Model Architecture and Training Configuration . . . . .	46
5.4.1	3D-CNN Model Architecture . . . . .	46
5.4.2	Optimisation and Training . . . . .	47
5.5	Federated Learning Strategies . . . . .	49
5.6	Evaluation Methodology . . . . .	49
5.6.1	Methodological Validation Protocol . . . . .	49
5.6.2	Performance Metrics . . . . .	50
5.6.3	Cross-Validation Protocol . . . . .	52
5.7	Summary . . . . .	52
<b>6</b>	<b>Results and Discussions</b>	<b>53</b>

6.1	Centralised vs Federated Performance Comparison . . . . .	53
6.1.1	Federated Learning Algorithm Performance . . . . .	53
6.1.2	Confusion Matrix Analysis . . . . .	54
6.1.3	ROC Curve Analysis . . . . .	55
6.1.4	Impact of number of clients in FL . . . . .	56
6.2	Differential Privacy Performance Evaluation . . . . .	57
6.2.1	Traditional Local Differential Privacy Results . . . . .	57
6.2.2	Adaptive Local Differential Privacy Results . . . . .	58
6.2.3	Training Dynamics: Fixed-Noise DP vs. Adaptive DP . . . . .	59
6.2.4	Privacy-Utility Trade-off Analysis . . . . .	61
6.3	Ablation Study: Impact of Individual Client Contributions in 4-Client Scenario . . . . .	62
6.3.1	Individual Performance Analysis and Collaborative Benefits . . . . .	63
6.3.2	Implications for Federated Learning Deployment . . . . .	63
6.4	Computational Efficiency of Federated Learning: Training Time Analysis . . . . .	63
6.4.1	Impact of Model Quantisation on Training Efficiency . . . . .	64
6.4.2	Standard Federated Learning Performance . . . . .	65
6.4.3	Privacy Mechanism Computational Overhead . . . . .	65
6.5	Discussions . . . . .	65
<b>7</b>	<b>Conclusions and Future Work</b>	<b>67</b>
7.1	Limitations . . . . .	67
7.2	Conclusions . . . . .	68
7.3	Future Work . . . . .	69
	<b>Bibliography</b>	<b>71</b>
<b>A</b>	<b>Appendix</b>	<b>77</b>
A.1	Key Hyperparameters for Federated Learning Training . . . . .	77
A.2	FedProx $\mu$ Finetuning . . . . .	78

## LIST OF FIGURES

2.1	Traditional centralised training paradigm in medical AI. Multiple healthcare institutions aggregate sensitive patient data in centralised repositories, creating privacy risks, regulatory compliance challenges, and single points of failure that limit collaborative medical AI development. . . . .	9
2.2	Federated learning paradigm for privacy-preserving collaborative medical AI. Healthcare institutions maintain local data sovereignty whilst participating in collaborative model development through secure parameter aggregation, eliminating the need for centralised data repositories whilst preserving privacy and regulatory compliance. . . . .	11
3.1	Overview of federated learning with Adaptive Local Differential Privacy (ALDP) in multi-institutional medical imaging. Each medical institution trains a local 3D CNN model on its private MRI data and applies local differential privacy by adding calibrated Gaussian noise to model parameters before transmission. In ALDP, both the privacy budget $\epsilon_t$ and noise scale $\sigma_{\text{base}}$ are adapted per round and per parameter tensor to improve privacy-utility trade-off. After each round, noisy local model updates are transmitted to a central server, where federated averaging is performed and the aggregated global model is broadcast back to all participating clients. . .	26
4.1	Implementation architecture for federated learning-based ADNI classification system. The framework integrates the Flower federated learning platform with MONAI medical imaging capabilities and PyTorch deep learning infrastructure. The modular design supports multiple federated learning strategies and enables both local simulation and distributed deployment across cloud servers for large-scale experiments. Comprehensive experiment tracking and monitoring are provided through Weights & Biases integration. . . . .	34

5.1 ADNI dataset filtering process using Analysis Ready Cohort (ARC) Builder on ida.loni.usc.edu platform, showing selection criteria for 3T MRI acquisitions and demographic filtering parameters. . . . . 40

5.2 Overview of the ADNI MRI image preprocessing pipeline. The workflow comprises: (1) downloading raw DICOM files; (2) converting DICOM series to volumetric NIfTI format; (3) resampling to 1 mm<sup>3</sup> isotropic voxel spacing for spatial consistency; (4) non-linear spatial normalization to the ICBM152 MNI template for anatomical alignment across subjects; and (5) skull stripping to remove non-brain tissue. This multi-step pipeline ensures each image is harmonised and analysis-ready for robust multi-site neuroimaging studies. . . . . 42

6.1 Normalized confusion matrices comparing centralised training with the best-performing federated approach. . . . . 55

6.2 ROC curves comparing centralised training with the best-performing federated approach. . . . . 56

6.3 Training loss curves for client 1 under  $(\epsilon, \delta)$ -differential privacy with fixed-noise DP, evaluated for varying  $\epsilon$  values (100, 500, 1000, 2000) over 100 rounds. For smaller  $\epsilon$ , the loss consistently increases, while for larger  $\epsilon$  improvement stalls or reverses in later rounds, illustrating the pitfall of fixed-noise schedules. . . . . 60

6.4 Training loss curves for client 1 under Adaptive  $(\epsilon, \delta)$ -DP with the same  $\epsilon_{\text{init}}$  as Figure 6.3. Loss decreases more consistently, confirming improved convergence and signal retention. . . . . 61

**LIST OF TABLES**

4.1	Comparative analysis of some prominent federated learning frameworks based on ease of use, documentation quality, features, community support, and overall score from Riedel et al. [40]. . . . .	32
5.1	Development dataset statistics showing distribution of subjects across diagnostic categories for training and validation . . . . .	43
5.2	Independent test dataset statistics showing balanced distribution across diagnostic categories for final evaluation . . . . .	43
5.3	3D CNN (CNN_8CL) architecture for 3D ADNI MRI classification . . . . .	46
6.1	Cross-validation results on the test set of the 3D CNN model under centralised and 2/3/4-client settings . . . . .	53
6.2	Comparative performance of Local $(\epsilon, \delta)$ -DP and Adaptive Local $(\epsilon, \delta)$ -DP (ALDP) strategies across varying numbers of clients and epsilon values, with $\delta$ fixed at $1 \times 10^{-5}$ and the clipping norm set to 1.0 for all experiments. . . . .	58
6.3	Results of an ablation study assessing the impact of individual client contributions in a federated learning setting. Each client was trained independently using only its own dataset, without data sharing, and evaluated on the same balanced test set (50 CN and 50 AD samples) as the global test set in the federated learning experiment presented in Table 6.1. The final column reports centralized training results, combining data from all four clients, which demonstrates improved performance through data aggregation. . . . .	62
6.4	Average total training time comparison across centralised and federated learning strategies (on 4-client scenario) for 100 training rounds/epochs. Results represent mean values computed from five independent experimental runs for each strategy.	64
A.1	Key Hyperparameters for Federated Learning Training . . . . .	77

A.2 Hyper-parameter tuning results for FedProx across different numbers of clients,  
illustrating the effect of varying  $\mu$  values on global test accuracy and F1 score. . . 78

## 1 INTRODUCTION

Federated learning represents a paradigm shift in collaborative machine learning that enables institutions to jointly develop robust AI models whilst maintaining complete data sovereignty and privacy protection. This distributed learning approach addresses one of the most pressing challenges in modern healthcare: leveraging the collective knowledge embedded in distributed medical datasets without compromising patient privacy or violating regulatory requirements. The significance of this paradigm is particularly pronounced in medical imaging applications, where the development of accurate diagnostic systems requires large, diverse datasets that individual institutions typically cannot provide in isolation.

This dissertation focuses specifically on privacy-preserving federated learning for Alzheimer's disease classification using three-dimensional magnetic resonance imaging (3D MRI) data from the Alzheimer's Disease Neuroimaging Initiative (ADNI). The research addresses critical gaps in existing federated learning methodologies through novel algorithmic contributions and comprehensive empirical evaluation, establishing a foundation for practical deployment of collaborative medical AI systems in real-world healthcare environments. The work encompasses theoretical innovations in privacy-preserving mechanisms, realistic evaluation methodologies, and systematic benchmarking of advanced federated learning strategies specifically tailored for high-dimensional medical imaging applications.

### 1.1 Background and Context

The convergence of artificial intelligence and healthcare has created unprecedented opportunities for improving diagnostic accuracy and patient outcomes through data-driven insights [38, 45]. Medical imaging, particularly neuroimaging for neurodegenerative disease detection, represents one of the most promising domains for AI applications due to the rich, high-dimensional information contained in brain scans [28]. However, the full potential of medical AI remains fundamentally constrained by data fragmentation, with valuable datasets isolated across institutional boundaries due to privacy regulations, competitive concerns, and technical barriers [37].

Traditional centralised approaches to medical AI development face insurmountable privacy and regulatory challenges under frameworks such as the Health Insurance Portability and Account-

ability Act (HIPAA) and the General Data Protection Regulation (GDPR) [21]. These regulations impose strict requirements for data sharing and processing that often preclude the centralised aggregation necessary for conventional machine learning approaches. Moreover, medical imaging data retains sufficient unique characteristics to enable patient re-identification even after removal of explicit identifiers, creating fundamental tensions between collaborative AI development and privacy preservation [42].

Federated learning has emerged as the most promising solution to these challenges, enabling collaborative model development across distributed data sources without requiring centralised data aggregation [30, 20]. Early applications in healthcare have demonstrated feasibility across various medical domains, including electronic health record analysis, medical imaging, and genomics research [41]. However, existing implementations suffer from significant limitations including unrealistic evaluation methodologies, inadequate privacy mechanisms, and insufficient algorithmic benchmarking under realistic multi-institutional conditions.

The application of federated learning to neuroimaging-based Alzheimer’s disease detection represents a particularly active area of research, with recent studies demonstrating promising results [32, 24]. Nevertheless, several critical gaps persist: (1) artificial data partitioning strategies that fail to preserve institutional boundaries, (2) limited exploration of differential privacy mechanisms for high-dimensional medical imaging, (3) lack of adaptive privacy approaches that account for training dynamics, and (4) insufficient systematic comparison of advanced federated learning algorithms under realistic conditions. These limitations have prevented the practical deployment of privacy-preserving federated learning in medical imaging applications where both diagnostic accuracy and formal privacy guarantees are essential requirements.

## 1.2 Objectives

This research addresses the identified gaps through novel methodological contributions and comprehensive empirical evaluation. The primary objectives of this dissertation are:

- **Develop a site-aware data partitioning methodology** that preserves institutional boundaries during federated learning evaluation, enabling realistic assessment of algorithm performance under conditions that reflect actual multi-institutional collaborations.

- **Design and implement an Adaptive Local Differential Privacy (ALDP) mechanism** that dynamically adjusts privacy parameters based on training progress and parameter characteristics, addressing fundamental limitations of fixed-noise approaches in high-dimensional medical imaging applications.
- **Conduct the first exploration of differential privacy mechanisms** for Alzheimer’s disease classification using ADNI neuroimaging data, establishing empirical guidelines for privacy-utility trade-offs in neuroimaging applications.
- **Implement and benchmark comprehensive federated learning strategies** including FedAvg, FedProx, and SecAgg+ protocols under realistic multi-institutional conditions, providing quantitative performance comparisons across multiple client configurations.

The technical implementation of these objectives involved developing a comprehensive software framework integrating the Flower federated learning platform with MONAI medical imaging capabilities and PyTorch deep learning infrastructure. The experimental evaluation encompassed systematic comparison across multiple client configurations (2, 3, and 4 clients) with comprehensive performance metrics including accuracy, F1 scores, confusion matrix analysis, and computational efficiency assessments.

### 1.3 Achievements

This dissertation makes several significant contributions to the field of privacy-preserving federated learning for medical imaging applications:

**Novel Adaptive Privacy Mechanism with Superior Performance:** The development of Adaptive Local Differential Privacy (ALDP) represents a significant improvement in privacy-preserving medical imaging, achieving 5-7 percentage point improvements over fixed-noise local differential privacy approaches. ALDP demonstrates remarkable performance at  $\epsilon_0 = 2000$ , reaching  $80.4 \pm 0.80\%$  accuracy—counter-intuitively exceeding the non-private centralised baseline ( $78.6 \pm 3.38\%$ ) while maintaining formal privacy guarantees. This exceptional result demonstrates the beneficial regularisation effects of adaptive noise injection in limited medical datasets, with superior convergence stability evidenced by exceptionally low variance (0.80%) compared to traditional DP’s high variance and training divergence.

**Systematic Privacy-Utility Analysis for Neuroimaging on ADNI dataset:** This work presents the comprehensive exploration of differential privacy mechanisms specifically applied to ADNI neuroimaging data for Alzheimer’s disease classification. The systematic evaluation across multiple privacy budgets and client configurations establishes quantitative benchmarks for privacy-preserving collaborative learning in healthcare, revealing temporal dynamics where ALDP maintains stable training while traditional fixed-noise approaches exhibit systematic convergence failures. The formal privacy guarantees combined with improved utility provide a practical solution for regulatory compliance in medical AI deployment.

**Empirical Evidence for Real-World Healthcare Deployment:** FedProx demonstrates superior performance over centralised training in realistic multi-institutional scenarios, achieving  $81.4 \pm 3.2\%$  accuracy compared to  $80.2 \pm 2.2\%$  in the 3-client configuration. Critically, FedProx significantly improves Alzheimer’s disease sensitivity from 64% to 74%—a clinically vital improvement for early detection and intervention. The comprehensive ablation study reveals substantial collaborative benefits, with individual client performance ranging from 68.2%-75.4% compared to the federated collaborative achievement of 81.4%, providing compelling evidence that privacy-preserving federated learning can enhance rather than compromise diagnostic performance in realistic healthcare environments.

**Methodological Innovation for Realistic Evaluation:** The introduction of site-aware data partitioning addresses a fundamental limitation in federated learning research by preserving institutional boundaries during evaluation, enabling more realistic assessment of multi-institutional collaboration challenges. This methodological contribution, combined with comprehensive algorithmic benchmarking across FedAvg, FedProx, and secure aggregation protocols, establishes a robust framework for evaluating federated learning approaches under conditions that reflect actual healthcare deployment scenarios.

These achievements collectively demonstrate that privacy-preserving federated learning can deliver clinically superior diagnostic performance while maintaining rigorous privacy guarantees, establishing a foundation for practical deployment in real-world healthcare collaborations.

#### 1.4 Overview of Dissertation

This dissertation is organised into seven chapters that systematically develop and evaluate the proposed methodological contributions:

**Chapter 1: Introduction** establishes the research context and motivation, outlining the fundamental challenges of data fragmentation in medical AI and positioning federated learning as a solution. The chapter presents the research objectives and summarises the key contributions achieved.

**Chapter 2: Background Theory and Literature Review** provides comprehensive theoretical foundations spanning medical AI challenges, federated learning algorithms, and privacy-preserving technologies. The chapter systematically identifies critical gaps in existing literature that motivate the novel methodological contributions presented in subsequent chapters.

**Chapter 3: Methodology** presents the core algorithmic innovations including the site-aware data partitioning strategy and the Adaptive Local Differential Privacy mechanism. The chapter provides detailed algorithmic specifications and theoretical justifications for the proposed approaches, establishing the foundation for experimental evaluation.

**Chapter 4: Implementation and Integration** describes the comprehensive software architecture that transforms theoretical contributions into a practical research platform. The chapter details framework selection criteria, system architecture design, and integration strategies that enable systematic experimental evaluation.

**Chapter 5: Experimental Setup** establishes the rigorous experimental protocol including ADNI dataset preprocessing, federated learning configurations, and evaluation methodologies. The chapter ensures reproducible experimental conditions whilst maintaining realistic multi-institutional scenarios through site-aware partitioning.

**Chapter 6: Results and Discussions** presents comprehensive experimental findings across four key areas: baseline performance comparisons, privacy-utility trade-off analysis, algorithmic robustness evaluation, and computational efficiency assessment. Results demonstrate the effectiveness of proposed methodological contributions through systematic empirical validation.

**Chapter 7: Conclusions and Future Work** synthesises research findings, discusses limitations and practical implications, and identifies directions for future research. The chapter positions the contributions within the broader context of privacy-preserving collaborative medical AI development.

The dissertation narrative progresses logically from theoretical foundations through methodological innovation to comprehensive empirical validation, providing both novel algorithmic contributions and practical solutions for privacy-preserving federated learning in medical imaging applications.

## **2 BACKGROUND THEORY AND LITERATURE REVIEW**

This chapter provides a comprehensive examination of the theoretical foundations and existing literature that underpin federated learning for privacy-preserving medical artificial intelligence, with particular emphasis on neuroimaging applications. The chapter systematically builds from fundamental concepts in medical AI and privacy challenges through to advanced federated learning techniques, establishing the theoretical groundwork and identifying critical gaps that motivate our research contributions. By synthesising existing knowledge across machine learning, medical informatics, privacy-preserving technologies, and neuroimaging, this review demonstrates the need for novel approaches to privacy-preserving collaborative medical AI and positions our methodological innovations within the broader research landscape.

### **2.1 Medical AI and the Challenge of Data Fragmentation**

Artificial intelligence has emerged as a transformative force in modern healthcare, with applications spanning diagnostic imaging, clinical decision support, drug discovery, and personalised medicine [38, 45]. The convergence of advanced machine learning algorithms, increased computational power, and the digitisation of healthcare data has created unprecedented opportunities for improving patient outcomes through data-driven insights. However, the full potential of medical AI remains fundamentally constrained by the fragmented nature of healthcare data, with valuable datasets isolated across institutional boundaries due to privacy regulations, competitive concerns, and technical barriers [37].

This fragmentation is particularly pronounced in neuroimaging, where the development of robust AI systems requires large, diverse datasets that capture the full spectrum of anatomical and pathological variations. Individual institutions typically possess datasets that, whilst clinically valuable, are insufficient in size and diversity to train state-of-the-art deep learning models. The resulting "data silos" prevent the realisation of AI systems that could benefit from the collective knowledge embedded in distributed medical datasets [21].

#### **2.1.1 Neuroimaging and Alzheimer's Disease Classification**

Neuroimaging represents one of the most promising yet challenging domains for medical AI applications. The rich, high-dimensional nature of brain imaging data provides detailed insights into

neuroanatomical structure and function, making it invaluable for diagnosing neurodegenerative diseases such as Alzheimer’s Disease (AD) [28]. The clinical significance of accurate early-stage AD detection cannot be overstated, as it enables timely intervention strategies that can significantly improve patient quality of life and potentially slow disease progression [19].

Traditional diagnostic approaches rely primarily on clinical assessment and neuropsychological testing, which may lack sensitivity in detecting subtle early-stage neurodegeneration [24]. Machine learning techniques applied to structural magnetic resonance imaging (MRI) data have demonstrated superior performance in distinguishing between diagnostic categories, with modern convolutional neural networks achieving classification accuracies exceeding 90% in controlled research settings [28]. However, these impressive results have been achieved primarily through centralised training approaches that aggregate data from multiple institutions, raising significant privacy and regulatory concerns that limit real-world deployment.

The Alzheimer’s Disease Neuroimaging Initiative (ADNI) exemplifies both the potential and limitations of current approaches to medical AI development. This landmark initiative has provided a standardised, multi-site dataset comprising over 1,000 T1-weighted MRI scans across diagnostic categories, enabling significant advances in neuroimaging-based classification [49]. Yet ADNI’s success required extensive data sharing agreements, standardised protocols, and centralised data repositories that may not be feasible for broader clinical deployment or international collaborations.

## **2.2 Privacy and Regulatory Challenges in Centralised Medical AI**

The centralised paradigm that has dominated medical AI research faces increasingly insurmountable privacy and regulatory challenges. Healthcare data is inherently sensitive and subject to stringent protection requirements under frameworks such as the Health Insurance Portability and Accountability Act (HIPAA) in the United States and the General Data Protection Regulation (GDPR) in the European Union [37]. These regulations impose strict requirements for data sharing, processing, and storage that often preclude the centralised aggregation necessary for traditional machine learning approaches.

### **2.2.1 Technical and Legal Barriers to Data Sharing**

The technical challenges of medical data sharing extend beyond simple regulatory compliance. Medical imaging data, particularly neuroimaging, retains sufficient unique characteristics to en-

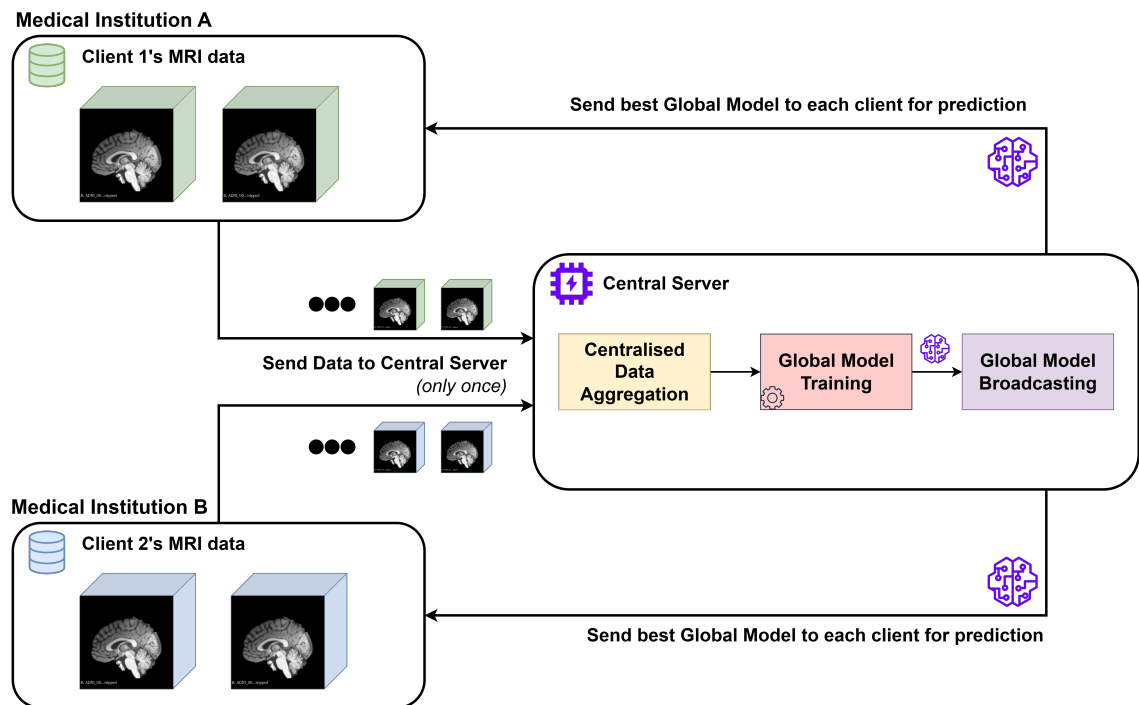


Figure 2.1: Traditional centralised training paradigm in medical AI. Multiple healthcare institutions aggregate sensitive patient data in centralised repositories, creating privacy risks, regulatory compliance challenges, and single points of failure that limit collaborative medical AI development.

able patient re-identification even after removal of explicit identifiers [42]. Brain anatomy exhibits individual-specific patterns that can serve as biometric identifiers, creating a fundamental tension between the data sharing necessary for AI development and privacy preservation requirements [12].

Data Use Agreements (DUAs) represent the current standard approach to enabling limited medical data sharing for research purposes. However, these legal instruments often require months-long approval processes, impose restrictive conditions on data usage, and typically limit sharing to specific research questions and timeframes [16]. The resulting fragmentation prevents the development of large-scale collaborative initiatives that could significantly advance medical AI capabilities whilst maintaining the flexibility necessary for iterative model development and validation.

International collaborations face additional complexity due to varying regulatory frameworks across jurisdictions. What constitutes acceptable privacy protection in one country may be insufficient in another, making it practically impossible to establish centralised repositories that satisfy all applicable requirements for global collaborative research [25].

### 2.2.2 Security Risks and Data Breach Implications

Beyond regulatory compliance, centralised medical data repositories present attractive targets for malicious actors. The healthcare sector has experienced a substantial increase in cyberattacks, with data breaches imposing significant financial and reputational costs [18]. The centralised nature of traditional AI development amplifies these risks, as a single successful attack can compromise vast quantities of sensitive patient information from multiple institutions.

These considerations have motivated exploration of alternative approaches to medical AI development that can harness the collective value of distributed datasets whilst addressing privacy, security, and regulatory concerns. Federated learning has emerged as the most promising paradigm for achieving this balance.

## 2.3 Theoretical Foundations of Federated Learning

Federated learning represents a paradigm shift in machine learning that enables collaborative model development across distributed data sources without requiring centralised data aggregation [30]. The fundamental principle underlying federated learning is the inversion of the traditional data science workflow: instead of bringing data to algorithms, federated learning brings algorithms to data, enabling computation on decentralised datasets whilst preserving data locality.

### 2.3.1 Core Components and Communication Protocols

The federated learning paradigm comprises three primary components: participating clients (representing individual institutions or data holders), a central aggregation server, and communication protocols that facilitate secure model parameter exchange [20]. This architecture enables institutions to collaborate on model development without compromising data sovereignty or violating privacy regulations.

### 2.3.2 Federated Averaging (FedAvg)

Federated Averaging (FedAvg) is the foundational algorithm in federated learning, enabling collaborative model optimization across clients without centralizing raw data [30]. In FedAvg, each client independently trains the global model on its local dataset for multiple epochs and then sends the resulting local model parameters to a central server. The server performs weighted averaging of these parameters based on the relative data sizes of the clients to obtain the updated global model, which is then redistributed for the next communication round.

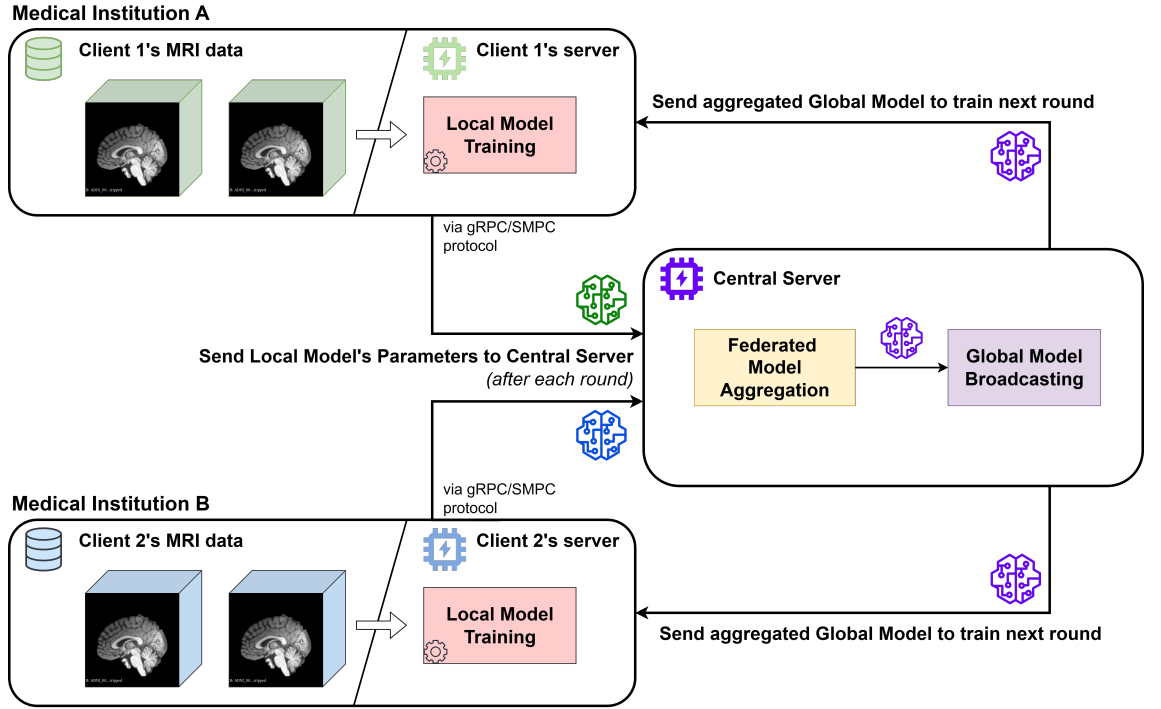


Figure 2.2: Federated learning paradigm for privacy-preserving collaborative medical AI. Healthcare institutions maintain local data sovereignty whilst participating in collaborative model development through secure parameter aggregation, eliminating the need for centralised data repositories whilst preserving privacy and regulatory compliance.

The aggregation update is defined as:

$$w_{t+1} = \sum_{k=1}^K \frac{n_k}{n} w_k^{t+1} \quad (2.1)$$

where  $w_{t+1}$  represents the global model parameters at round  $t + 1$ ,  $w_k^{t+1}$  denotes the local model parameters from client  $k$  after local training,  $n_k$  is the number of samples at client  $k$ , and  $n = \sum_{k=1}^K n_k$  represents the total number of samples across all clients.

FedAvg is widely adopted for its simplicity and communication efficiency. However, it assumes that local data distributions are similar (i.e., independently and identically distributed - IID), which is often not the case in real-world medical imaging federations, leading to potential issues with model convergence and accuracy [43].

### 2.3.3 Federated Proximal (FedProx)

Federated Proximal (FedProx) extends FedAvg to better address statistical heterogeneity across clients in federated learning scenarios [26]. In practice, differences in patient demographics, imag-

ing protocols, and institutional environments frequently lead to non-IID data distributions, causing local model updates to diverge from the global optimum.

FedProx modifies the local objective function by adding a proximal term, which regularizes each client’s update to remain closer to the current global model:

$$\min_w F_k(w) + \frac{\mu}{2} \|w - w^t\|^2 \quad (2.2)$$

where  $F_k(w)$  denotes the local empirical loss for client  $k$ ,  $w$  is the model parameter vector,  $w^t$  is the global model parameter from the previous round, and  $\mu$  is a hyperparameter controlling the regularisation strength.

By penalizing large deviations from the global model, FedProx improves training stability in the presence of non-IID data and client drift, helping federated learning systems converge more robustly in heterogeneous medical imaging environments.

While these algorithms enable collaborative training, they must be augmented with privacy-preserving technologies to address residual vulnerabilities in medical applications.

## 2.4 Privacy-Preserving Technologies for Federated Learning

Whilst federated learning provides inherent privacy benefits by avoiding centralised data aggregation, model parameters can still leak sensitive information about training data through various attack vectors [53]. Membership inference attacks can determine whether specific individuals participated in model training, whilst model inversion attacks can reconstruct training data from model parameters [46]. These vulnerabilities necessitate additional privacy-preserving mechanisms to achieve formal privacy guarantees.

### 2.4.1 Local DP: Differential Privacy in Federated Learning

Local Differential Privacy (Local DP) is a privacy-preserving mechanism in federated learning that ensures each participating institution shares only obfuscated information with the server, thus maintaining data sovereignty and compliance with strict privacy regulations [11]. LDP adds calibrated noise *directly to the locally updated model parameters* before transmission to the server. This approach is particularly suitable for medical imaging federations where sensitive raw images

never leave the client devices, and additional privacy guarantees are required for regulatory or ethical reasons [21, 42].

Formally, each client’s model parameters  $\theta$  are perturbed as follows before aggregation:

$$\tilde{\theta} = \theta + \mathcal{N}(0, \sigma^2 \mathbf{I}) \quad (2.3)$$

where  $\mathcal{N}(0, \sigma^2 \mathbf{I})$  is a multivariate Gaussian noise with zero mean and variance  $\sigma^2$  calibrated according to the desired  $(\epsilon, \delta)$ -differential privacy parameters. The noise scale  $\sigma$  is typically determined by the sensitivity of the model parameters and the specified privacy budget, following the Gaussian mechanism:

$$\sigma = \frac{\Delta}{\epsilon} \sqrt{2 \ln(1.25/\delta)} \quad (2.4)$$

where  $\Delta$  is the sensitivity (e.g., determined by norm clipping),  $\epsilon$  denotes the privacy budget, and  $\delta$  is a small failure probability.

This Local DP mechanism ensures that each client’s contribution is *differentially private* at the point of sharing, independent of the server and other participants. Model aggregation is then performed by the server on these noisy parameters.

This approach offers several benefits in federated medical imaging:

- **Strong client autonomy:** All noise is added locally, so trust in the server is not required.
- **Simplicity:** No changes are required to the local optimization process or deep learning pipeline.
- **Regulatory alignment:** Since only noised models are ever shared, data subjects benefit from provable privacy guarantees atop institutional data silos.

However, adding sufficient noise for stringent privacy can degrade model performance, especially in high-dimensional applications such as 3D neuroimaging. Therefore, choosing the appropriate noise scale and developing adaptive strategies (as further explored in this work) is critical for maintaining the utility of privacy-preserving federated learning in medical domains.

## 2.4.2 SecAgg+: Secure Aggregation Protocols

Secure aggregation provides complementary privacy protection by ensuring that individual client updates remain confidential even from the aggregation server [7]. This additional layer of protection addresses residual privacy vulnerabilities that persist when merely sharing model parameters, such as membership inference and model inversion attacks, which are particularly concerning in healthcare and neuroimaging contexts.

The standard secure aggregation protocol operates in three key phases:

1. **Setup:** Clients coordinate the generation and distribution of cryptographic keys and secret shares necessary for the subsequent masking process.
2. **Masking:** Prior to transmission, each client applies a cryptographic mask to its model updates, utilising threshold secret sharing schemes. This ensures that, without a coalition of clients, the server cannot reconstruct any individual update.
3. **Unmasking and Aggregation:** Upon receipt, the server is able to recover only the sum of the masked updates, as the cryptographic masks effectively cancel each other, thus revealing the aggregate but not the individual contributions.

Whilst this protocol offers robust privacy guarantees compatible with regulatory requirements, its computational and communication overhead increases substantially with larger client pools and high-dimensional models typical in medical imaging. As a result, scalability and efficiency remain significant challenges when deploying secure aggregation in practical medical AI systems.

SecAgg+ advances this foundational protocol in several important respects [5]. By introducing optimised threshold secret sharing, SecAgg+ tolerates client dropouts, maintaining privacy and correctness in aggregation even under realistic network conditions. Furthermore, it employs improved quantisation and clipping approaches tailored for high-dimensional deep learning models, substantially reducing bandwidth requirements without compromising privacy. More efficient key exchange and secret splitting mechanisms facilitate scalability, enabling robust secure aggregation across larger federations and complex neuroimaging models.

Collectively, these enhancements render SecAgg+ a practical solution for privacy-preserving federated learning in medical applications, supporting secure collaboration for use cases such as

multi-institutional Alzheimer’s disease classification with volumetric MRI data, whilst remaining feasible under real-world resource constraints.

## **2.5 Federated Learning in Healthcare: Current State and Limitations**

The application of federated learning to healthcare has gained significant momentum, driven by the compelling need to leverage distributed medical data whilst maintaining privacy compliance [41]. Early applications have demonstrated feasibility across various medical domains, including electronic health record analysis, medical imaging, drug discovery, and genomics research.

### **2.5.1 Medical Imaging Applications**

Within medical imaging, federated learning has shown promise for diverse tasks including chest X-ray analysis for COVID-19 detection, brain tumour segmentation, diabetic retinopathy screening, and skin lesion classification [27]. These applications have demonstrated that federated approaches can achieve performance comparable to centralised methods whilst addressing institutional data sharing constraints.

However, most existing implementations focus on simulated federated scenarios rather than realistic multi-institutional deployments. The controlled nature of these studies, whilst valuable for algorithmic development, limits insight into the practical challenges of real-world federated learning deployment in healthcare environments.

### **2.5.2 Neuroimaging and Alzheimer’s Disease Detection**

The application of federated learning to neuroimaging-based Alzheimer’s disease detection represents a particularly active area of research. Mitrovska et al. [32] demonstrated the feasibility of secure federated learning for AD classification using structural MRI data, comparing federated averaging and secure aggregation against centralised training baselines. Their work established important foundations but focused primarily on basic algorithmic comparisons rather than comprehensive privacy-utility trade-off analysis.

Lei et al. [24] extended this foundation with a hybrid federated learning framework incorporating brain-region attention mechanisms for enhanced interpretability. Their approach demonstrated state-of-the-art performance whilst providing insights into the neuroanatomical basis of classification decisions.

Despite these advances, several critical limitations persist in current federated neuroimaging research:

**Unrealistic Data Partitioning:** Most studies use artificially shuffled data partitions that fail to preserve institutional boundaries, creating unrealistic scenarios that do not reflect the natural heterogeneity found in multi-institutional collaborations.

**Limited Privacy Mechanisms:** Most implementations rely on basic federated aggregation without formal privacy guarantees. Few studies have explored differential privacy mechanisms on neuroimaging datasets, particularly for Alzheimer’s disease classification.

**Inadequate Algorithmic Benchmarking:** Limited systematic comparison of different federated learning algorithms makes it difficult to establish best practices or guide algorithmic choices for practitioners.

## 2.6 Research Gaps and Opportunities

Despite significant progress in federated learning and privacy-preserving machine learning, several critical gaps remain in their application to medical imaging, particularly for neuroimaging-based disease classification. These gaps represent both challenges and opportunities for advancing the field toward practical deployment in real-world healthcare settings.

### 2.6.1 Site-Aware Data Partitioning for Realistic Federated Scenarios

The first major gap concerns the unrealistic data partitioning strategies employed in most federated learning studies. Current approaches typically use random data shuffling across clients, which fails to preserve the natural institutional boundaries and statistical heterogeneity that characterise real-world multi-institutional collaborations [20]. This artificial partitioning creates overly optimistic evaluation scenarios that do not reflect the challenges of actual federated deployments.

In real-world medical federated learning, each participating institution contributes its complete local dataset, which typically exhibits site-specific characteristics related to patient demographics, acquisition protocols, and clinical practices. These institutional differences create natural statistical heterogeneity that significantly impacts federated learning performance but is not captured by random data partitioning approaches.

The medical imaging community would benefit significantly from rigorous evaluation protocols that preserve institutional boundaries during data partitioning, enabling more realistic assessment of federated learning performance under conditions that reflect practical deployment scenarios. Such evaluation protocols should maintain complete site integrity whilst ensuring balanced participation across clients.

### **2.6.2 Differential Privacy Exploration for Neuroimaging Applications**

The second critical gap involves the lack of systematic exploration of differential privacy mechanisms specifically for neuroimaging-based disease classification. Whilst differential privacy has been extensively studied in general machine learning contexts, its application to high-dimensional medical imaging data, particularly for Alzheimer’s disease detection using ADNI data, remains largely unexplored.

This gap is particularly significant given the sensitivity of medical imaging data and the stringent privacy requirements in healthcare applications. The unique characteristics of 3D neuroimaging data—including high dimensionality, spatial correlations, and anatomical constraints—create specific challenges for privacy-preserving techniques that have not been systematically addressed in existing literature.

The exploration of differential privacy on ADNI neuroimaging data represents a novel contribution that could provide valuable insights into the practical feasibility of privacy-preserving collaborative learning in neuroscience research. Such exploration should systematically evaluate the utility-privacy trade-offs specific to neuroimaging applications whilst establishing empirical guidelines for parameter selection.

### **2.6.3 Adaptive Privacy Mechanism Development**

The third gap concerns the limitations of static differential privacy approaches when applied to iterative machine learning processes such as federated learning. Standard differential privacy mechanisms apply fixed noise levels throughout training, failing to account for the temporal dynamics of model optimisation and the varying sensitivity of different neural network parameters.

Traditional fixed-epsilon differential privacy approaches often result in excessive utility degradation when applied to high-dimensional imaging data due to the substantial noise injection required to maintain formal privacy guarantees [42]. This limitation has prevented the practical

deployment of privacy-preserving federated learning in medical imaging applications where diagnostic accuracy requirements are stringent.

The development of adaptive differential privacy mechanisms that can dynamically adjust privacy parameters based on training progress and parameter characteristics represents a significant opportunity for improving utility-privacy trade-offs. Such mechanisms should account for both temporal training dynamics and the heterogeneous nature of neural network parameters whilst maintaining rigorous privacy guarantees.

#### **2.6.4 Algorithmic Benchmarking of Advanced Strategies**

The fourth gap relates to the absence of benchmarking studies that evaluate a range of advanced federated learning algorithms within realistic medical imaging contexts. Much of the existing research [32, 27, 24] either assesses federated approaches in isolation or restricts analyses to direct comparisons between only two algorithms. This approach makes it challenging to discern the relative strengths and weaknesses of more recent federated learning strategies—such as FedProx and SecAgg+ protocols—when confronted with the unique challenges posed by heterogeneous, multi-institutional neuroimaging data.

The diversity of available federated learning algorithms—including FedAvg, FedProx, and various secure aggregation protocols—combined with the unique characteristics of medical imaging data suggests that comprehensive benchmarking studies could provide valuable guidance for practitioners. Such studies should evaluate algorithms across multiple dimensions including accuracy, communication efficiency, robustness to statistical heterogeneity, and compatibility with privacy-preserving mechanisms.

### **2.7 Positioning of Current Research**

The gaps identified in existing literature motivate our research contributions, which address three key limitations in federated learning for medical imaging through novel methodological innovations and systematic empirical evaluation.

**Site-Aware Data Splitting Methodology:** Our research introduces a novel site-aware data partitioning strategy that preserves institutional boundaries during federated learning evaluation, providing more realistic assessment of algorithm performance under conditions that reflect actual

multi-institutional collaborations. This approach addresses the fundamental limitation of random data shuffling by maintaining complete site integrity whilst ensuring balanced client participation.

**First Systematic Exploration of Differential Privacy on ADNI Data:** We conduct the first comprehensive investigation of differential privacy mechanisms specifically for Alzheimer’s disease classification using ADNI neuroimaging data. This exploration systematically evaluates utility-privacy trade-offs under realistic federated scenarios, providing novel insights into the practical feasibility of privacy-preserving neuroimaging applications.

**Adaptive Local Differential Privacy (ALDP):** Our research introduces a novel adaptive differential privacy mechanism that dynamically adjusts privacy parameters based on training progress and parameter characteristics. ALDP addresses the fundamental limitations of fixed-epsilon approaches through temporal privacy budget scheduling and per-tensor variance-aware noise scaling, enabling significantly improved utility-privacy trade-offs for high-dimensional medical imaging data.

**Evaluating Advanced Federated Learning Strategies:** We extend previous baselines [32] by implementing and benchmarking recent advanced federated learning algorithms, including FedProx and SecAgg+, on the ADNI neuroimaging dataset using our site-aware partitioning methodology. This enables direct assessment of their performance and robustness under realistic multi-institutional conditions, providing valuable insights into the effectiveness of these state-of-the-art approaches in handling statistical heterogeneity in medical imaging.

These contributions advance the state-of-the-art in privacy-preserving federated learning for medical imaging whilst providing practical solutions that enable more realistic evaluation and improved privacy-utility trade-offs. The combination of methodological innovations and systematic empirical evaluation establishes a foundation for future research in privacy-preserving collaborative medical AI.

## 2.8 Chapter Summary

This literature review has established the theoretical foundations and identified critical research gaps that motivate our work on federated learning for privacy-preserving medical AI. The review reveals that whilst significant progress has been made in applying federated learning to medi-

cal imaging, fundamental challenges remain regarding realistic evaluation methodologies, privacy mechanism adaptation, and systematic algorithmic assessment.

Traditional centralised approaches to medical AI development face insurmountable privacy and regulatory barriers that prevent their adoption in real-world clinical settings. Federated learning emerges as a promising solution, but current approaches suffer from limitations in evaluation realism, privacy mechanism exploration, and algorithmic benchmarking.

The gaps identified in existing literature—particularly regarding site-aware data partitioning, differential privacy exploration on neuroimaging data, adaptive privacy mechanisms, and comprehensive algorithmic benchmarking—provide clear motivation for the methodological innovations presented in the following chapter.

Our research addresses these limitations through: (1) novel site-aware data splitting that preserves institutional boundaries, (2) the first systematic exploration of differential privacy on ADNI data, (3) adaptive differential privacy mechanisms with temporal and parameter-aware scaling, and (4) comprehensive benchmarking of federated learning algorithms under realistic conditions.

By addressing these fundamental gaps, our research contributes to making privacy-preserving federated learning viable for medical imaging applications whilst providing more realistic evaluation methodologies and improved privacy-utility trade-offs essential for practical deployment.

The next chapter details the comprehensive methodology developed to address these challenges, including our novel site-aware partitioning strategy, systematic differential privacy exploration, adaptive privacy mechanisms, and benchmarking framework for neuroimaging-based Alzheimer’s disease classification.

### 3 METHODOLOGY

This chapter presents the comprehensive methodological framework developed for federated learning-based Alzheimer’s disease classification using ADNI MRI data with integrated privacy-preserving mechanisms. The methodology addresses critical gaps identified in the literature review (see Chapter 2): inadequate simulation of real-world data heterogeneity, lack of adaptive privacy mechanisms for high-dimensional medical imaging, and insufficient integration of advanced privacy-preserving techniques in federated AI.

#### 3.1 Site-Aware Data Partitioning: Realistic Federated Learning Simulation

A fundamental gap in existing federated learning evaluation methodology on ADNI dataset is the failure to preserve realistic data heterogeneity patterns that characterize real-world multi-institutional collaborations. Traditional approaches employ random data partitioning across simulated clients, artificially mixing samples from different institutions and obscuring the natural statistical heterogeneity that drives performance differences in practical federated deployments [43]. Our research addresses this limitation through the development of a novel site-aware data partitioning strategy that maintains institutional boundaries while ensuring balanced client participation.

##### 3.1.1 Motivation and Problem Formulation

The ADNI dataset naturally exhibits multi-site heterogeneity, with data collected across multiple research institutions using varying acquisition protocols, scanner configurations, and patient populations. This heterogeneity reflects realistic federated learning scenarios where participating institutions contribute their complete local datasets rather than artificially shuffled subsets of a global dataset.

Traditional random partitioning strategies fail to capture these realistic conditions by:

- **Artificial mixing** of samples from different sites within the same federated client
- **Loss of institutional characteristics** that drive real-world non-IID conditions

- **Underestimation** of performance challenges associated with true multi-institutional collaboration
- **Reduced generalizability** of results to practical deployment scenarios

### 3.1.2 Site-Aware Distribution Algorithm

Our site-aware distribution strategy preserves institutional boundaries while ensuring balanced participation across federated clients. The algorithm employs a greedy load-balancing approach that operates in two distinct phases:

---

#### Algorithm 1: Site-Aware Data Partitioning for Federated Learning

---

**Input:** Dataset  $\mathcal{D}$  with site labels  $S$ , number of clients  $K$ , train ratio  $r$ , random seed  $\text{seed}$

**Output:** Client datasets  $\{\mathcal{D}_k^{\text{train}}, \mathcal{D}_k^{\text{val}}\}_{k=1}^K$

// Phase 1: Site Analysis and Ranking

site\_counts  $\leftarrow$  ComputeRecordCountsPerSite( $S$ )

sorted\_sites  $\leftarrow$  SortDescending(site\_counts)

// Phase 2: Greedy Client Assignment

Initialize client\_assignments  $\leftarrow \{\emptyset\}_{k=1}^K$

Initialize client\_sizes  $\leftarrow \{0\}_{k=1}^K$

**for** each site  $s$  in sorted\_sites **do**

$k^* \leftarrow \arg \min_k \text{client\_sizes}[k]$  // Client with fewest samples

client\_assignments[ $k^*$ ]  $\leftarrow$  client\_assignments[ $k^*$ ]  $\cup$  { $s$ }

client\_sizes[ $k^*$ ]  $\leftarrow$  client\_sizes[ $k^*$ ] + site\_counts[ $s$ ]

// Phase 3: Train-Validation Splitting per Client

Set random seed to  $\text{seed}$

**for** each client  $k$  **do**

$\mathcal{D}_k \leftarrow$  FilterBySites( $\mathcal{D}$ , client\_assignments[ $k$ ])

$\mathcal{D}_k \leftarrow$  ShuffleData( $\mathcal{D}_k$ ,  $\text{seed}$ )

split\_idx  $\leftarrow \lfloor |\mathcal{D}_k| \times r \rfloor$

$\mathcal{D}_k^{\text{train}} \leftarrow \mathcal{D}_k[0 : \text{split\_idx}]$

$\mathcal{D}_k^{\text{val}} \leftarrow \mathcal{D}_k[\text{split\_idx} : ]$

**return**  $\{\mathcal{D}_k^{\text{train}}, \mathcal{D}_k^{\text{val}}\}_{k=1}^K$

---

### 3.1.3 Methodological Advantages

The site-aware partitioning strategy provides several critical advantages for federated learning research in medical imaging:

**Preserved Site Integrity:** No institution’s data is fragmented across multiple federated clients, maintaining the natural clustering of patient populations, acquisition protocols, and institutional practices that characterize real-world collaborative scenarios.

**Realistic Non-IID Evaluation:** Each federated client represents distinct institutional characteristics, enabling more accurate assessment of federated learning performance under realistic data heterogeneity conditions typical of multi-institutional medical collaborations.

**Enhanced Generalizability:** Results obtained through site-aware partitioning provide stronger evidence for the practical applicability of federated learning approaches in real-world deployment scenarios where institutional data sovereignty must be maintained.

**Load-Balanced Participation:** The greedy assignment algorithm ensures approximately equal sample distribution across clients while preserving site boundaries, preventing scenarios where certain clients are disadvantaged due to small dataset sizes.

This methodological innovation addresses a fundamental limitation in federated learning evaluation that has limited the practical applicability of research findings to real-world deployment scenarios. Complementing this realistic data distribution, we next address privacy challenges through a novel adaptive mechanism tailored for high-dimensional medical data.

## 3.2 Adaptive Local Differential Privacy: A Novel Privacy Mechanism

The development of effective privacy-preserving mechanisms for high-dimensional medical imaging represents the primary methodological innovation of this research. Standard differential privacy approaches face significant challenges when applied to 3D medical imaging data, where the substantial noise injection required to maintain formal privacy guarantees often results in prohibitive utility degradation [42]. Our research addresses this fundamental limitation through the development of an Adaptive Local Differential Privacy (ALDP) mechanism that introduces temporal and parameter-aware noise scaling.

### 3.2.1 Motivation: Limitations of Fixed-Noise Differential Privacy

Traditional Local DP implementations in federated learning typically apply a fixed noise schedule throughout the entire training process, failing to accommodate the dynamic evolution of gradient magnitudes and parameter sensitivities during deep learning optimization. This rigid approach, while guaranteeing that prescribed privacy constraints are never violated, can severely undermine model performance and limit practical applicability, especially for high-dimensional medical imaging data.

Several adaptive approaches to differential privacy have been proposed to overcome the limitations of fixed noise injection. For instance, Fu et al. [15] introduced Adap DP-FL, a framework for differentially private federated learning with *adaptive noise*, aiming to improve the privacy-utility balance by tuning the noise based on training dynamics. Similarly, Kiani et al. [22] proposed a method for *time-adaptive privacy spending*, which modulates the local privacy budget over the course of training to better match the evolving sensitivity of model parameters.

Despite these advances, existing works have focused either on adapting privacy at each training round (temporal adaptation) or on dynamically adjusting the noise level. However, none of these prior methods jointly incorporate both (1) temporal adaptation—modulating privacy and noise over the course of training—and (2) parameter-awareness—modifying noise per-parameter according to tensor statistics. The ALDP mechanism presented here is a novel solution that fills this critical gap by simultaneously adjusting the privacy budget across rounds and scaling noise injection based on the statistical characteristics of each parameter tensor. This dual adaptation enables rigorous privacy guarantees tailored for high-dimensional medical data, while mitigating utility degradation that typically plagues fixed-noise approaches.

- **Temporal Misalignment:** Early training phases can tolerate higher noise due to large gradient magnitudes, but late-stage learning requires careful noise scaling to preserve important fine-tuning signals.
- **Parameter Heterogeneity:** Uniform noise injection often overwhelms small-magnitude parameters and under-regularizes high-variance ones.

- **Utility Degradation:** Without adaptive mechanisms, model performance is significantly compromised, limiting the practical deployment of privacy-preserving federated learning for diagnostic medical imaging. A concrete illustration of these effects is provided in Figure 6.3.

By addressing both temporal and parameter-scale adaptation, the ALDP mechanism advances state-of-the-art privacy-preserving techniques in federated learning and provides an essential methodological innovation for multi-institutional collaborative AI in healthcare.

### 3.2.2 ALDP Algorithm

The schematic in Figure 3.1 provides a visual summary of how privacy-preserving mechanisms are integrated into multi-institutional federated learning for high-dimensional medical imaging. In this workflow, each medical institution independently trains a local 3D CNN on private MRI data. Before sharing model updates, each client applies local differential privacy (Local DP), either through a traditional fixed-noise mechanism or a novel adaptive strategy (ALDP), as depicted in the upper-left inset of the diagram.

The ALDP mechanism addresses these limitations through two complementary innovations: exponential privacy budget growth scheduling and per-tensor variance-aware noise scaling.

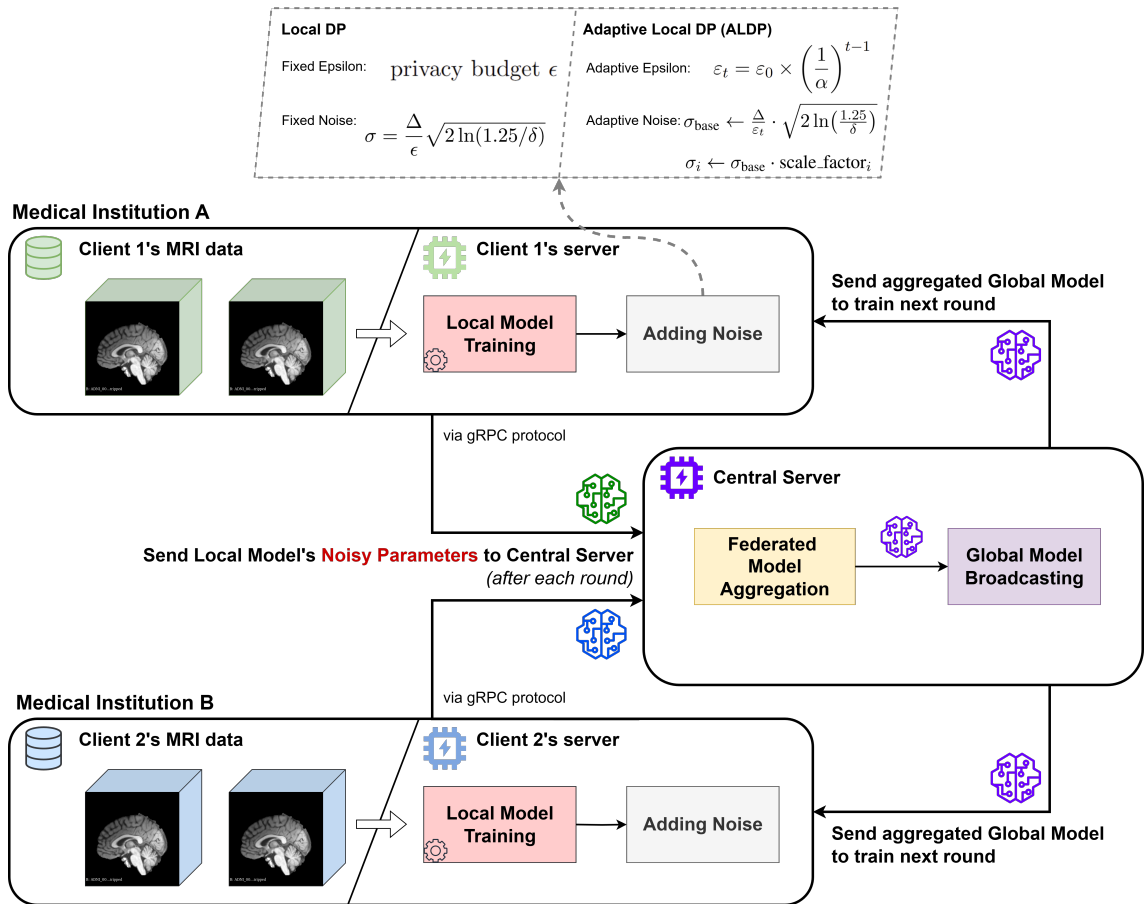


Figure 3.1: Overview of federated learning with Adaptive Local Differential Privacy (ALDP) in multi-institutional medical imaging. Each medical institution trains a local 3D CNN model on its private MRI data and applies local differential privacy by adding calibrated Gaussian noise to model parameters before transmission. In ALDP, both the privacy budget  $\epsilon_t$  and noise scale  $\sigma_{\text{base}}$  are adapted per round and per parameter tensor to improve privacy-utility trade-off. After each round, noisy local model updates are transmitted to a central server, where federated averaging is performed and the aggregated global model is broadcast back to all participating clients.

**Algorithm 2:** Adaptive Local Differential Privacy with Gaussian Noise Scaling

**Input:**  $C$  (clipping norm as sensitivity),  $\varepsilon_0$  (initial privacy budget),  $\delta$  (privacy parameter),

$\alpha \in (0, 1)$  (decay factor),  $\varepsilon_{\min}$  (minimum budget),  $\varepsilon_{\max}$  (maximum budget)

**Output:** Noisy parameters  $\tilde{\Theta} = \{\tilde{\theta}_i\}_{i=1}^{|\Theta|}$

// Initialize

$\Delta \leftarrow C$  // Use clipping norm as sensitivity

$t \leftarrow 0$  // Current round

**for** each federated learning round **do**

$t \leftarrow t + 1$

    // Exponential epsilon growth

$\varepsilon_t \leftarrow \varepsilon_0 \cdot \left(\frac{1}{\alpha}\right)^{t-1}$

    // Clamp privacy budget

$\varepsilon_t \leftarrow \max(\min(\varepsilon_t, \varepsilon_{\max}), \varepsilon_{\min})$

    // Gaussian base noise scale for  $(\varepsilon_t, \delta)$ -DP

$\sigma_{\text{base}} \leftarrow \frac{\Delta}{\varepsilon_t} \cdot \sqrt{2 \ln\left(\frac{1.25}{\delta}\right)}$

    // Compute per-tensor statistics once

$\{\text{std}_i\}_{i=1}^{|\Theta|} \leftarrow \{\text{StandardDeviation}(\theta_i)\}$

$\overline{\text{std}} \leftarrow \max\left(\frac{1}{|\Theta|} \sum_{i=1}^{|\Theta|} \text{std}_i, 10^{-12}\right)$

    // Apply adaptive Gaussian noise

**for**  $i = 1$  **to**  $|\Theta|$  **do**

$\text{rel\_std}_i \leftarrow \frac{\text{std}_i}{\overline{\text{std}}}$

$\text{scale\_factor}_i \leftarrow \text{CLIP}(\text{rel\_std}_i, 0.1, 1.0)$

$\sigma_i \leftarrow \sigma_{\text{base}} \cdot \text{scale\_factor}_i$

$\mathcal{N}_i \sim \mathcal{N}(0, \sigma_i^2 \mathbf{I})$

$\tilde{\theta}_i \leftarrow \theta_i + \mathcal{N}_i$

**return**  $\tilde{\Theta} = \{\tilde{\theta}_i\}_{i=1}^{|\Theta|}$

// Privacy guarantee:  $(\varepsilon_t, \delta)$  per round with Gaussian noise

// Adaptive properties: Temporal noise reduction +

per-tensor scaling

### 3.2.3 Temporal Privacy Budget Adaptation

The temporal adaptation component implements exponential privacy budget growth according to:

$$\varepsilon_t = \varepsilon_0 \times \left(\frac{1}{\alpha}\right)^{t-1} \quad (3.1)$$

where  $\varepsilon_t$  represents the privacy budget at round  $t$ ,  $\varepsilon_0$  is the initial budget, and  $\alpha$  controls the rate of budget expansion. This schedule provides strong privacy protection during early training rounds when models are learning fundamental patterns, gradually relaxing constraints as models approach convergence and gradient magnitudes naturally decrease.

The privacy budget is bounded by minimum and maximum thresholds to ensure both privacy preservation and practical utility:

$$\varepsilon_t = \max(\min(\varepsilon_t, \varepsilon_{\max}), \varepsilon_{\min}) \quad (3.2)$$

### 3.2.4 Per-Tensor Variance-Aware Noise Scaling

The parameter adaptation component calibrates noise injection based on the statistical properties of individual parameter tensors:

$$\sigma_i = \sigma_{\text{base}} \times \text{clip}\left(\frac{\text{std}_i}{\overline{\text{std}}}, 0.1, 1.0\right) \quad (3.3)$$

where  $\sigma_i$  is the adapted noise scale for tensor  $i$ ,  $\text{std}_i$  is the standard deviation of tensor  $i$ , and  $\overline{\text{std}}$  is the mean standard deviation across all tensors. The clipping operation ensures that small-variance parameters receive at least 10% of the base noise level while preventing excessive noise scaling for high-variance parameters.

This dual adaptation mechanism enables ALDP to maintain meaningful privacy guarantees whilst significantly improving model utility compared to fixed-noise approaches, particularly for high-dimensional medical imaging applications where parameter heterogeneity is pronounced.

## 3.3 Summary

This methodology chapter has presented the comprehensive framework for privacy-preserving federated learning research in medical imaging, with particular emphasis on novel methodological contributions that address critical gaps in existing approaches. The framework integrates two

primary innovations: site-aware data partitioning that preserves realistic institutional heterogeneity, and adaptive local differential privacy mechanisms that optimize privacy-utility trade-offs for medical imaging data.

The site-aware partitioning strategy represents a fundamental advance in federated learning evaluation methodology, ensuring that research findings reflect the challenges and opportunities inherent in real-world multi-institutional collaborations. The ALDP mechanism provides a practical solution to the privacy-utility dilemma that has limited the adoption of privacy-preserving techniques in medical imaging, enabling formal privacy guarantees without prohibitive performance degradation.

The methodological framework establishes theoretical foundations that are systematically implemented and evaluated in the following chapters. Chapter 4 details the implementation architecture that realises these methodological innovations within a practical research framework, while Chapter 5 presents the experimental protocols that enable rigorous evaluation of these contributions using the ADNI neuroimaging dataset.

The combination of novel theoretical contributions and systematic empirical evaluation enables this research to advance the state-of-the-art in privacy-preserving collaborative medical AI while providing practical guidelines for real-world deployment in healthcare environments. The methodological innovations presented establish a foundation for more realistic and privacy-preserving approaches to federated learning in medical imaging that can facilitate broader adoption of collaborative AI in healthcare settings.

## 4 IMPLEMENTATION AND INTEGRATION

This chapter presents the engineering architecture that enables systematic evaluation of privacy-preserving federated learning algorithms for medical imaging applications. The implementation transforms the theoretical methodological contributions presented in Chapter 3 into a practical, scalable research platform specifically designed for ADNI neuroimaging data. The architecture integrates federated learning algorithms with medical imaging preprocessing pipelines and privacy-preserving mechanisms, enabling rigorous experimental evaluation whilst maintaining privacy compliance and realistic multi-institutional scenarios.

The complete implementation used in this dissertation was coded from scratch and is publicly available at: [github.com/Tin-Hoang/fl-adni-classification](https://github.com/Tin-Hoang/fl-adni-classification). To reproduce the main experiments, see the repository’s README and `configs/` directory. We provide pinned environments, fixed random seeds, and scripts to launch centralised and federated runs.

The implementation follows a modular design philosophy that separates concerns between federated learning orchestration, medical data processing, privacy mechanism integration, and experimental evaluation. This separation enables systematic comparison of different algorithmic approaches whilst maintaining the flexibility necessary for iterative research development and the reproducibility essential for scientific validation.

### 4.1 FL Framework Selection

The selection of appropriate software frameworks and implementation strategies plays a crucial role in the success of federated learning research in medical imaging.

#### 4.1.1 Selection Criteria and Justification

The framework selection was based on several key criteria essential for privacy-preserving federated learning research in medical imaging:

**Algorithmic Flexibility:** The framework must support systematic comparison of multiple federated learning algorithms (FedAvg, FedProx, SecAgg+) within a unified experimental environment to allow a comprehensive comparison of our methodological contributions.

**Privacy Integration:** Native support for differential privacy mechanisms and extensibility for novel privacy approaches (such as our ALDP mechanism) is essential for implementing comprehensive privacy-preserving federated learning.

**Medical Imaging Compatibility:** Integration capabilities with specialised medical imaging frameworks (such as MONAI) and support for high-dimensional 3D medical data processing pipelines.

**Research-Oriented Design:** Robust simulation capabilities that enable controlled experimentation while maintaining realistic federated learning conditions, particularly important for systematic evaluation of site-aware partitioning strategies.

Based on the comprehensive analysis by Riedel et al. [40], who evaluated 15 open-source federated learning frameworks on features, interoperability, and user-friendliness, the Flower framework was selected as the foundation for this research, achieving the highest score (84.75%) among available alternatives.

#### 4.1.2 Flower Framework Advantages for Medical Imaging Research

The Flower framework’s superiority for this research stems from several key advantages particularly relevant for medical imaging applications [40]:

**Comprehensive Strategy Pattern Implementation:** Flower’s modular architecture enables systematic comparison of multiple federated learning algorithms (FedAvg, FedProx, SecAgg+) within a unified experimental framework, essential for the benchmarking objectives of this research.

**Controlled Simulation Environment:** The framework provides robust simulation capabilities that enable systematic evaluation of federated learning algorithms under controlled conditions while maintaining realistic client heterogeneity patterns. This is crucial for research scenarios where comprehensive experimental control is required to isolate the impact of different algorithmic and privacy choices.

**Privacy Integration Capabilities:** Native support for differential privacy mechanisms through integration with privacy libraries enables seamless implementation of both standard Local DP and novel adaptive privacy mechanisms within the federated learning pipeline.

Table 4.1: Comparative analysis of some prominent federated learning frameworks based on ease of use, documentation quality, features, community support, and overall score from Riedel et al. [40].

Framework	Easy to use	Documentation	Features	Community	Score
Flower	Highly user-friendly with intuitive APIs and extensive tutorials.	Comprehensive and well-maintained with numerous tutorials.	Cross-device FL, scalable client-server architecture, FedAvg/SecAgg/DP support, PyTorch integration	6200+ GitHub stars, 164+ contributors. Active community.	84.75%
PySyft	Steeper learning curve for beginners.	Some documentation may be outdated or less detailed.	Privacy-focused (DP, SMPC), encrypted computation, PyTorch-based	9600+ GitHub stars, 428+ contributors.	72.5%
OpenFL	Balanced between ease of use and robustness for research and production.	Decent documentation covering installation, tutorials, and API references.	Workflow-based FL, enterprise-ready, model aggregation, PyTorch and TensorFlow support.	2000+ GitHub stars, 164+ contributors.	69%
NVFlare	Production-focused with good documentation, suitable for users familiar with FL concepts.	Detailed documentation with guides for getting started and advanced topics.	Privacy-preserving FL, large file streaming, multi-cloud support, FedAvg/FedProx	700+ GitHub stars, 46+ contributors.	80.5%

**Medical Imaging Framework Integration:** Extensive compatibility with PyTorch and specialized medical imaging frameworks such as MONAI enables sophisticated preprocessing pipelines specifically designed for 3D neuroimaging data [9].

Our implementation leverages Flower’s modular architecture to develop a comprehensive federated learning framework specifically optimised for ADNI neuroimaging data. The system integrates advanced preprocessing capabilities through the Medical Open Network for AI (MONAI) framework, which provides specialised transforms and data handling optimised for 3D medical imaging [16].

## 4.2 Medical Imaging Framework Integration

The implementation integrates specialised medical imaging capabilities through the Medical Open Network for Artificial Intelligence (MONAI) framework [9]. MONAI provides domain-specific transforms, data handling routines, and preprocessing pipelines optimised for 3D medical imaging applications, enabling sophisticated augmentation strategies specifically designed for brain MRI data.

The MONAI integration enables several critical capabilities:

**Domain-Specific Preprocessing:** Specialised transforms for medical imaging data, including intensity normalisation, spatial resampling, and anatomically aware augmentation techniques that maintain clinical relevance while providing robust data augmentation for limited-size medical datasets.

**Format Compatibility:** Native support for medical imaging formats including DICOM and NIfTI, eliminating the need for custom data loading and conversion routines whilst ensuring compatibility with established neuroimaging analysis pipelines.

**Performance Optimization:** GPU-accelerated preprocessing and augmentation operations that enable efficient handling of high-dimensional 3D volumetric data typical of neuroimaging applications.

## 4.3 System Architecture Overview

The implementation leverages Flower’s modular architecture to develop a comprehensive research framework specifically optimised for ADNI neuroimaging data [6]. The system architecture, illustrated in Figure 4.1, integrates four core components that address the unique requirements of privacy-preserving federated learning in medical imaging applications: the federated learning core, medical imaging pipeline, deployment infrastructure, and experiment tracking systems.

This modular design enables flexible experimentation across diverse federated learning configurations whilst maintaining consistent evaluation protocols and ensuring reproducible results across different deployment scenarios.

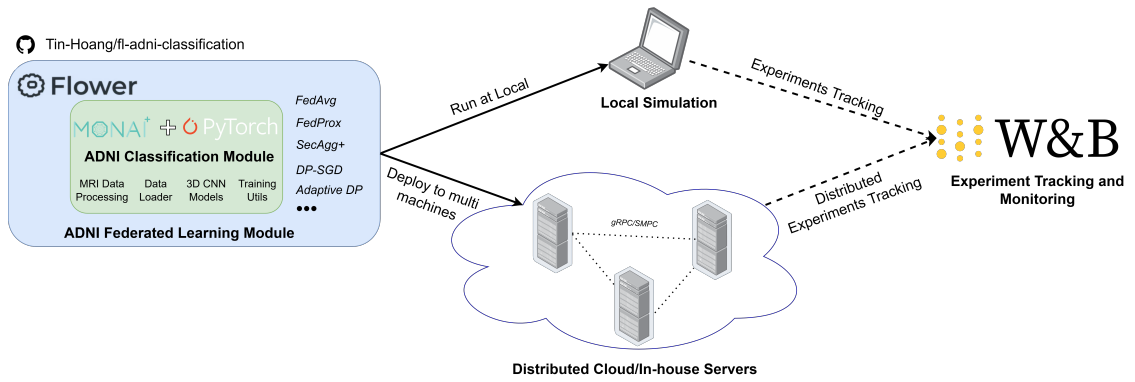


Figure 4.1: Implementation architecture for federated learning-based ADNI classification system. The framework integrates the Flower federated learning platform with MONAI medical imaging capabilities and PyTorch deep learning infrastructure. The modular design supports multiple federated learning strategies and enables both local simulation and distributed deployment across cloud servers for large-scale experiments. Comprehensive experiment tracking and monitoring are provided through Weights & Biases integration.

### 4.3.1 Integration and Coordination Principles

The architectural integration follows several design principles essential for rigorous federated learning research in medical imaging applications, ensuring that experimental results provide meaningful insights into practical deployment scenarios.

**Modular Design:** Component independence enables systematic evaluation of individual methodological contributions whilst maintaining overall system coherence. This modularity supports iterative development and enables isolated testing of novel algorithmic components without compromising system stability.

**Controlled Heterogeneity:** Site-aware partitioning integration ensures that client heterogeneity reflects realistic multi-institutional scenarios whilst maintaining experimental control necessary for systematic algorithm comparison [43]. This approach preserves natural statistical heterogeneity characteristic of real-world medical collaborations whilst enabling controlled evaluation of algorithmic performance.

**Reproducible Evaluation:** Deterministic data partitioning and seeded random number generation ensure experimental reproducibility whilst comprehensive logging captures detailed metrics for post-hoc analysis. The framework incorporates rigorous validation protocols that account for stochastic variability in data partitioning and model initialisation, ensuring statistical validity of performance comparisons.

### 4.3.2 Federated Learning Core

The federated learning core implements Flower’s strategy pattern architecture to provide systematic comparison capabilities across multiple federated learning algorithms and privacy mechanisms. This component serves as the central orchestration layer that coordinates distributed training whilst maintaining algorithmic consistency and experimental control.

**Multi-Strategy Support:** The core supports comprehensive evaluation of federated learning algorithms including FedAvg for baseline comparison, FedProx for addressing client heterogeneity, and privacy-enhanced variants incorporating both standard Local DP and novel ALDP mechanisms [30, 26, 1]. Each strategy is implemented with configurable parameters enabling systematic exploration of algorithmic trade-offs under realistic multi-institutional scenarios.

**Privacy Integration:** Comprehensive privacy mechanisms are integrated at multiple levels, including client-level differential privacy through Local DP and ALDP approaches, cryptographic protection through SecAgg+ protocols, and privacy accounting to ensure formal privacy guarantees throughout the federated training process [1, 7]. This multi-layered approach provides defence-in-depth protection for sensitive medical data during collaborative model development.

### 4.3.3 Medical Imaging Pipeline

The medical imaging pipeline integrates domain-specific preprocessing capabilities optimised for 3D neuroimaging data through seamless integration with the Medical Open Network for AI (MONAI) framework. This component addresses the unique challenges of federated medical imaging research whilst maintaining clinical relevance and diagnostic accuracy.

**MONAI Framework Integration:** Integration with MONAI transforms enables sophisticated augmentation strategies specifically designed for brain MRI data, including elastic deformations, bias field corrections, and Rician noise simulation [9, 16]. This integration ensures that data preprocessing maintains clinical relevance whilst providing sufficient augmentation to prevent overfitting in federated scenarios where individual client datasets may be limited in size.

**Privacy-Compatible Architectures:** The pipeline incorporates architectural modifications to support differential privacy requirements, including replacement of BatchNorm layers with GroupNorm to maintain per-sample gradient independence required for DP [51, 1]. This ensures compat-

ibility with privacy-preserving mechanisms without compromising the fundamental capabilities of 3D convolutional networks for neuroimaging analysis.

**Domain-Specific Processing:** The ADNI classification module implements specialised pre-processing pipelines for T1-weighted MRI data, including spatial normalisation, intensity harmonisation, and quality assurance protocols that maintain consistency across multi-institutional datasets whilst preserving anatomical integrity essential for accurate Alzheimer’s disease classification.

**Training Efficiency:** The framework incorporates mixed precision training to reduce memory usage and accelerate training on modern GPUs whilst maintaining model accuracy [31]. This optimization enables practical federated training of large 3D CNN models across distributed institutional networks with varying computational resources.

#### 4.3.4 Local and Distributed Deployment Infrastructure

The deployment infrastructure provides flexible execution capabilities supporting both local simulation for development and distributed deployment across cloud servers for large-scale experiments. This dual-deployment capability ensures scalable evaluation under realistic communication and computational constraints.

**Local Simulation Environment:** The framework provides robust local simulation capabilities enabling systematic evaluation of federated learning algorithms under controlled conditions whilst maintaining realistic client heterogeneity patterns. This environment is crucial for algorithm development, parameter tuning, and preliminary evaluation before distributed deployment.

**Distributed Cloud Deployment:** Multi-machine deployment capabilities through SSH-based distributed execution enable realistic evaluation under varying communication latencies and bandwidth constraints typical of healthcare research environments [23]. The distributed architecture supports scalable federated training across multiple cloud servers, simulating realistic multi-institutional network conditions.

**Fault Tolerance and Recovery:** The infrastructure incorporates comprehensive error handling and fault tolerance mechanisms, including checkpoint-based recovery and adaptive client selection, providing resilience against network interruptions or client resource limitations common in distributed healthcare research environments.

### 4.3.5 Experiment Tracking and Monitoring

The implementation integrates comprehensive monitoring and logging capabilities through Weights & Biases integration<sup>1</sup>, enabling detailed analysis of federated learning dynamics and experimental results:

**Real-Time Monitoring:** Live tracking of client-specific and aggregated performance metrics, including loss curves, accuracy progression, and convergence indicators, provides immediate feedback on training dynamics and enables early detection of performance issues or algorithmic failures.

**Algorithm Performance Analytics:** Comprehensive logging captures detailed metrics including client-specific performance characteristics, global validation accuracy, confusion matrix visualisation, sample debug images, communication overhead analysis essential for post-hoc analysis and algorithmic comparison across different federated learning strategies.

**System Performance Analytics:** Detailed logging of computational performance, network utilization, and resource consumption, enabling optimization of system performance and identification of bottlenecks in distributed deployments.

## 4.4 Summary

This implementation chapter has presented the comprehensive technical architecture that transforms the theoretical methodological contributions described in Chapter 3 into a practical, scalable research platform for privacy-preserving federated learning in medical imaging. The implementation successfully integrates multiple complex technologies—federated learning algorithms, medical imaging processing, privacy-preserving mechanisms, and distributed computing infrastructure—into a cohesive system that enables rigorous experimental evaluation whilst maintaining practical applicability.

The modular architecture ensures that individual components can be systematically evaluated and compared whilst maintaining overall system coherence. The integration of established frameworks (Flower, MONAI, PyTorch) with novel methodological contributions (ALDP, site-aware partitioning) provides a foundation for advancing the state-of-the-art in privacy-preserving collaborative medical AI whilst ensuring reproducibility and extensibility for future research.

---

<sup>1</sup>Weights & Biases project: <https://wandb.ai/tin-hoang/fl-adni-classification>

The comprehensive experimental design framework supports rigorous evaluation of our methodological contributions across multiple dimensions including algorithmic performance, privacy-utility trade-offs, and scalability under varying collaboration scales. The modular architecture enables systematic comparison of federated learning approaches whilst providing the experimental control necessary for drawing reliable conclusions about optimal strategies for privacy-preserving collaborative medical AI.

The implementation framework establishes the foundation for the comprehensive experimental evaluation presented in Chapter 5, where these systems are applied to systematic benchmarking of federated learning approaches for Alzheimer’s disease classification using the ADNI dataset. The combination of novel methodological contributions, comprehensive implementation architecture, and rigorous experimental design enables this research to advance the state-of-the-art in privacy-preserving federated learning whilst providing practical solutions for real-world deployment in healthcare environments.

## 5 EXPERIMENTAL SETUP

This section presents the comprehensive experimental framework designed to evaluate federated learning strategies for privacy-preserving Alzheimer’s disease classification using 3D MRI neuroimaging data. The experiments systematically compare multiple federated optimization algorithms against centralised training baselines across diverse institutional collaboration scenarios, with particular emphasis on realistic data distribution patterns that reflect real-world federated deployments in medical imaging.

The experimental design follows the methodological framework established by Mitrovska et al. [32], extending their approach with several key innovations: (1) site-aware data partitioning that preserves institutional data distribution patterns, and (2) comprehensive evaluation across multiple federated learning strategies including differential privacy and secure aggregation mechanisms. The experiments simulate realistic multi-institutional scenarios with 2, 3, and 4 participating clients, representing different scales of federated collaboration commonly encountered in medical imaging consortiums.

### 5.1 Dataset Acquisition and Preprocessing

#### 5.1.1 ADNI Data Collection

The experimental dataset was acquired from the Alzheimer’s Disease Neuroimaging Initiative (ADNI) database [35], a longitudinal multicentre study designed to develop clinical, imaging, genetic, and biochemical biomarkers for early detection and tracking of Alzheimer’s disease progression [33]. The dataset comprised 3T T1-weighted MRI scans in DICOM format, selected using the Analysis Ready Cohort (ARC) Builder interface on the IDA platform<sup>1</sup>.

#### 5.1.2 Image Preprocessing Pipeline

The ADNI image preprocessing pipeline followed established neuroimaging protocols to ensure spatial consistency, harmonise images across sites, and facilitate robust cross-institutional model training. This workflow, illustrated in Figure 5.2, comprised the following sequential steps:

<sup>1</sup><https://ida.loni.usc.edu/home/projectPage.jsp?project=ADNI>



Figure 5.1: ADNI dataset filtering process using Analysis Ready Cohort (ARC) Builder on [ida.loni.usc.edu](http://ida.loni.usc.edu) platform, showing selection criteria for 3T MRI acquisitions and demographic filtering parameters.

1. **Downloading DICOM files:** Raw MRI scans were collected in DICOM format from the ADNI repository. Each scan typically comprised 170–211 DICOM files per acquisition session, preserving the original image series.
2. **DICOM to NIfTI conversion:** Raw DICOM images for each subject were first converted to volumetric NIfTI format, yielding 3D brain images (dimensions  $\sim 176 \times 240 \times 256$  voxels) compatible with neuroimaging pipelines.
3. **Resampling to isotropic 1mm:** All NIfTI volumes were resampled to an isotropic voxel size of  $1 \text{ mm}^3$  (e.g.,  $211 \times 253 \times 270$  voxels) using ANTs' `ResampleImageBySpacing` tool. This standardisation of spatial resolution and orientation ( $176 \times 240 \times 256$  to  $211 \times 253 \times 270$  voxels) minimised site and scanner variability.
4. **Spatial normalization to MNI space:** All resampled images underwent nonlinear registration to the ICBM152 MNI template space [14, 13] using ANTs `antsRegistrationSyN.sh` with the symmetric normalisation (SyN) algorithm. This alignment ( $197 \times 233 \times 189$  voxels) enabled anatomically meaningful aggregation and model sharing across multi-site datasets [29].
5. **Skull stripping:** Non-brain tissue was removed using FSL's Brain Extraction Tool (BET) [44], with parameters (fractional intensity threshold  $f = 0.1$ , "B" option for bias field correction) optimised for ADNI and other multi-site studies [36]. The resulting images contained only standardised brain parenchyma, maximising data uniformity for downstream classification.

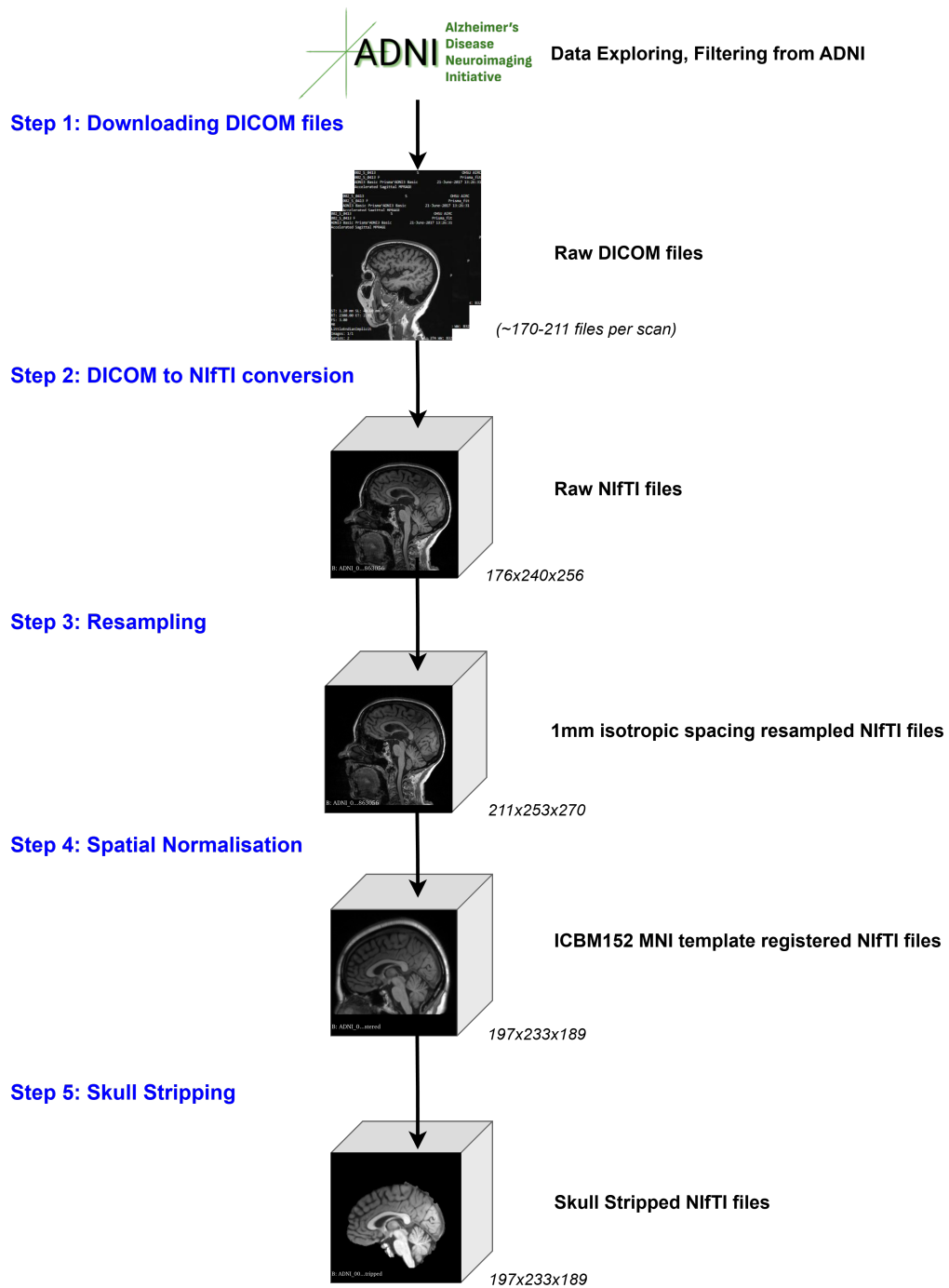


Figure 5.2: Overview of the ADNI MRI image preprocessing pipeline. The workflow comprises: (1) downloading raw DICOM files; (2) converting DICOM series to volumetric NIFTI format; (3) resampling to 1 mm<sup>3</sup> isotropic voxel spacing for spatial consistency; (4) non-linear spatial normalization to the ICBM152 MNI template for anatomical alignment across subjects; and (5) skull stripping to remove non-brain tissue. This multi-step pipeline ensures each image is harmonised and analysis-ready for robust multi-site neuroimaging studies.

### 5.1.3 Data Quality Assurance and Duplicate Removal

To address data leakage concerns identified in previous ADNI studies [50, 52], rigorous quality assurance procedures were implemented. Following the recommendations of Wen et al. [50], only a single scan at the baseline visit ("sc", "bl" or "init" suffix) were retained for each subject, eliminating temporal dependencies that could artificially inflate classification performance. Corrupted and duplicate images were systematically identified and removed through automated quality checks and manual verification.

## 5.2 Data Filtering and Label Conversion

### 5.2.1 Initial Dataset Composition

The downloaded ADNI dataset initially contained 1220 3D T1-weighted MRI images distributed across three diagnostic categories: Cognitively Normal (CN), Mild Cognitive Impairment (MCI), and Alzheimer's Disease (AD). The dataset exhibited class imbalance typical of clinical cohorts, with varying representation across diagnostic categories.

### 5.2.2 Label Conversion

Given the clinical focus on binary classification between cognitively normal individuals and those with Alzheimer's disease, the experimental framework adopted a two-class paradigm (CN vs. AD). To address the limited availability of AD cases and the clinical relevance of progression from MCI to dementia, selected MCI cases were reclassified based on established clinical progression patterns.

Following clinical staging criteria [4], MCI cases were subcategorised into: Significant Memory Concern (SMC), Early MCI (EMCI), and Late MCI (LMCI). Given the established progression pathway from EMCI through LMCI to AD, Late MCI (LMCI) cases were reclassified as AD, reflecting their high likelihood of progression to dementia within the study timeframe. This approach aligns with clinical practice where LMCI represents a prodromal stage of Alzheimer's disease.

### 5.2.3 Final Dataset Statistics

After data cleaning, quality assurance, and class balancing procedures, the final dataset was partitioned into development and evaluation subsets following established neuroimaging evaluation protocols. The development dataset, comprising 797 subjects for training and validation purposes,

maintained the clinical characteristics essential for robust Alzheimer’s disease classification whilst ensuring balanced representation across diagnostic categories.

Table 5.1: Development dataset statistics showing distribution of subjects across diagnostic categories for training and validation

Diagnosis	#Subjects	Gender (Male/Female)	Age (years)
Cognitively Normal (CN)	490	199/291	$70.58 \pm 6.62$
Dementia (AD)	307	174/133	$73.45 \pm 7.86$

The development dataset exhibited demographic characteristics typical of Alzheimer’s disease cohorts, with AD patients showing higher mean age compared to cognitively normal subjects, reflecting the age-related progression of neurodegeneration. The gender distribution favoured females in the CN group whilst maintaining relative balance in the AD group, consistent with epidemiological patterns observed in aging populations.

A separate held-out test set of 100 subjects (50 CN and 50 AD cases) was preserved following the evaluation protocol established by Mitrovska et al. [32], ensuring consistent comparison with baseline methodologies and preventing data leakage during model development. The test set maintained balanced representation across diagnostic categories whilst preserving demographic diversity essential for robust performance evaluation.

Table 5.2: Independent test dataset statistics showing balanced distribution across diagnostic categories for final evaluation

Diagnosis	#Subjects	Gender (Male/Female)	Age (years)
Cognitively Normal (CN)	50	15/35	$68.90 \pm 6.57$
Dementia (AD)	50	33/17	$73.97 \pm 7.62$

### 5.3 Federated Data Splitting: Multi-Client Scenarios

The experimental framework evaluates three distinct collaboration scales that represent common federated learning deployment scenarios in medical imaging consortiums:

- **2-Client Federation:** Simulating bilateral institutional collaboration, this scenario represents the simplest federated learning deployment where two major medical centres collaborate on model development whilst maintaining data sovereignty. This configuration enables evaluation of basic federated learning dynamics whilst minimising coordination complexity.

- **3-Client Federation:** Representing small consortium partnerships, this scenario models collaborations between research institutions that are common in medical imaging research. The three-client configuration enables evaluation of federated learning performance under moderate heterogeneity whilst maintaining manageable coordination overhead.
- **4-Client Federation:** Modelling larger multi-institutional networks, this scenario represents more complex federated deployments involving multiple healthcare systems or international collaborations. The four-client configuration enables evaluation of scalability and robustness under increased coordination complexity and data heterogeneity.

Each scenario maintains the site-aware distribution principle (see section 3.1) whilst ensuring balanced data allocation across participating clients, enabling systematic evaluation of how collaboration scale affects federated learning performance under realistic conditions.

### 5.3.1 On-the-fly Data Augmentation Strategy

Data augmentation addresses the fundamental challenge of overfitting inherent in small-scale medical imaging datasets, particularly within federated learning environments where individual client datasets are further constrained by institutional boundaries. The ADNI dataset, whilst clinically comprehensive, presents typical limitations of medical imaging studies with modest sample sizes (797 training images) that necessitate sophisticated augmentation strategies to achieve robust model generalisation [17]. This challenge is compounded in federated settings where participating sites may possess even smaller local datasets, making aggressive yet clinically appropriate augmentation essential for preventing overfitting whilst preserving diagnostic relevance.

The implemented augmentation pipeline utilises the Medical Open Network for Artificial Intelligence (MONAI) framework [9] with domain-specific transforms optimised for 3D medical imaging. The comprehensive strategy incorporates both geometric and intensity-based transformations, each selected to address specific aspects of medical imaging variability whilst enhancing model robustness in federated training scenarios.

**Geometric Transformations:** Random horizontal flipping (`RandFlipd`, 50% probability) simulates natural variations in patient positioning whilst preserving bilateral brain symmetry. In federated contexts, this transformation helps normalise site-specific positioning protocols and reduces institutional biases. Affine transformations (`RandAffined`) introduce controlled rotations

( $\pm 10^\circ$ ) and scaling variations ( $\pm 10\%$ ) that account for inter-subject morphological differences and scanner positioning variability [29]. These parameters were carefully constrained to remain within physiologically reasonable ranges whilst providing sufficient variation to prevent model memorisation.

**Elastic Deformations and Anatomical Variability:** Three-dimensional elastic transformations (`Rand3DElasticd`) with sigma range (3, 10) and magnitude range (3, 20) simulate realistic tissue deformations whilst preserving topological relationships essential for neuroanatomical analysis. These deformations combat overfitting by generating novel anatomical configurations that prevent memorisation of specific brain shapes whilst enhancing robustness against natural anatomical variations across institutional populations.

**MRI-Specific Intensity Augmentations:** The pipeline incorporates physics-based augmentations simulating common MRI acquisition artefacts. Bias field inhomogeneity simulation (`RandBiasFieldd`, 30% probability) models spatial intensity variations due to radiofrequency coil sensitivity patterns, crucial for federated scenarios where institutions employ scanners with varying configurations. Gibbs ringing artefacts (`RandGibbsNoised`, 20% probability) simulate k-space truncation effects that vary across acquisition protocols [10]. Rician noise simulation (`RandRicianNoised`, 30% probability) models the fundamental noise characteristics of magnitude MRI data, ensuring robustness against varying noise levels across scanner configurations.

**Combating Overfitting in Limited Data:** This aggressive augmentation strategy directly addresses the primary limitation of medical imaging datasets: insufficient sample diversity for robust deep learning. With approximately 797 images distributed across diagnostic categories, the filtered ADNI dataset poses significant overfitting risks for deep 3D CNNs with millions of parameters. The augmentation pipeline effectively multiplies the dataset size through stochastic combinations of transformations, each application generating clinically plausible yet novel brain volumes. This approach is particularly critical in federated settings where individual clients may possess 100-200 samples, making conventional training highly susceptible to overfitting.

**Federated Integration:** Each participating client applies identical augmentation protocols using site-specific random seeds, ensuring reproducibility whilst maintaining statistical independence across the federation. This standardises data enhancement procedures, reduces site-specific

overfitting likelihood, and maintains privacy-preserving nature by avoiding parameter sharing between sites.

## 5.4 Model Architecture and Training Configuration

### 5.4.1 3D-CNN Model Architecture

The experiments employed a domain-specific 3D convolutional neural network optimised for ADNI classification tasks from [47]. This architecture was selected based on its demonstrated effectiveness in Alzheimer’s disease detection and its focus on reproducible methodological practices in medical imaging.

The 3D CNN architecture features an 8-layer convolutional design with progressive channel expansion: [8, 8, 16, 16, 32, 32, 64, 64] channels, incorporating spatial pooling operations with kernel sizes  $(4, 4, 4) \rightarrow (3, 3, 3) \rightarrow (2, 2, 2) \rightarrow (2, 2, 2)$ . This configuration, matching the CNN\_8CL setup of [47], was specifically optimised for 3D brain MRI volumes with spatial dimensions (73, 96, 96), balancing model capacity with computational efficiency for federated training scenarios.

Table 5.3: 3D CNN (CNN\_8CL) architecture for 3D ADNI MRI classification

Layer	Type	Kernel Size	Pooling	Output Channels
Layer 1	Conv3d + BN + ReLU + MaxPool	(3,3,3)	(4,4,4)	8
Layer 2	Conv3d + BN + ReLU	(3,3,3)	-	8
Layer 3	Conv3d + BN + ReLU + MaxPool	(3,3,3)	(3,3,3)	16
Layer 4	Conv3d + BN + ReLU	(3,3,3)	-	16
Layer 5	Conv3d + BN + ReLU + MaxPool	(3,3,3)	(2,2,2)	32
Layer 6	Conv3d + BN + ReLU	(3,3,3)	-	32
Layer 7	Conv3d + BN + ReLU + MaxPool	(3,3,3)	(2,2,2)	64
Layer 8	Conv3d + BN + ReLU	(3,3,3)	-	64
Fully Connected	Linear	-	-	num_classes

Key architectural principles are:

- **3D Convolutions:** Each block preserves the volumetric structure, capturing spatially localized patterns crucial for neuroanatomical analysis.
- **Progressive Pooling:** Max pooling is strategically applied after selected blocks to reduce spatial resolution and enhance multiscale hierarchical feature abstraction, as reflected in the sequence of pooling operations in the code.

- **Batch Normalization:** BatchNorm is employed after each convolution, promoting convergence stability across distributed clients.
- **Dropout Regularization:** A configurable dropout is included after activations to mitigate overfitting during federated or data-limited training.

**Note on Differential Privacy Compatibility:** In the differential privacy experiments, the standard BatchNorm layers will be replaced by GroupNorm [51] layers due to BatchNorm’s incompatibility with DP [2]. BatchNorm creates cross-sample dependencies within batches, violating the per-sample gradient independence required for differential privacy guarantees. GroupNorm provides equivalent normalization benefits while maintaining sample independence.

### 5.4.2 Optimisation and Training

The training was designed for robust and scalable federated learning with thorough hyperparameter management, rapid convergence, and resilience to distributed systems issues.

Our optimisation pipeline used AdamW optimizer, with the learning rate typically initialized at  $1 \times 10^{-4}$  according to best practices for training 3D convolutional models from scratch. Training batch size was limited to 2–8 due to GPU memory constraints of 3D volumes, with gradient accumulation employed to achieve effective batch sizes up to 16 or higher for stable gradient updates and improved convergence under federated regimes.

**Loss Function and Class Imbalance Handling:** To address pronounced class imbalances typical in clinical datasets, the primary loss function employed was weighted cross-entropy. Given the development dataset distribution with 490 CN and 307 AD cases, class imbalance presented a significant challenge for model training. The weighted cross-entropy loss compensates for this imbalance by assigning higher penalties to misclassification of underrepresented classes, defined as:

$$L_{weighted} = -\frac{1}{N} \sum_{i=1}^N w_{y_i} \log(p_{y_i}) \quad (5.1)$$

where  $w_{y_i}$  represents the class weight for the true class  $y_i$ ,  $p_{y_i}$  is the predicted probability for the true class, and  $N$  is the total number of samples. Class weights were computed using inverse frequency weighting:

$$w_c = \frac{n_{total}}{n_{classes} \times n_c} \quad (5.2)$$

where  $n_{total}$  is the total number of samples,  $n_{classes}$  is the number of classes, and  $n_c$  is the number of samples in class  $c$ . This weighting strategy ensures that the minority class (AD) receives proportionally higher importance during training, preventing the model from developing a bias toward the majority class (CN).

**Learning Rate Scheduling and Regularisation:** The training employed cosine annealing learning rate scheduling to facilitate smooth convergence and prevent premature convergence to suboptimal solutions. Weight decay regularisation ( $1 \times 10^{-2}$ ) was applied to prevent overfitting, particularly crucial given the limited dataset size typical of medical imaging studies. Mixed precision training was utilised where computationally feasible to reduce memory usage and accelerate training on modern GPUs whilst maintaining model accuracy.

**Model Selection and Checkpointing:** Throughout training, model checkpoints were saved at regular intervals to enable model selection based on validation performance. For centralised training, validation accuracy was computed using the held-out validation set at the end of each epoch, with the best checkpoint selected based on peak validation performance. For federated learning experiments, the global model was evaluated every 5 federated rounds on an aggregated global validation set comprising the combination of all local validation sets from participating clients. The checkpoint achieving the highest accuracy on this aggregated validation set was selected as the final model, ensuring generalisation across all participating institutions whilst preventing overfitting—a critical consideration in medical imaging applications with limited dataset sizes.

Comprehensive convergence monitoring, including early stopping and dynamic learning rate scheduling, is performed globally and per client. All metrics, including client-specific and aggregated loss curves, parameter distribution summaries, privacy budget expenditure, and communication overhead, are tracked live using Weights & Biases <sup>2</sup>. Error handling and fault tolerance are

<sup>2</sup>Weights & Biases experiments: <https://wandb.ai/tin-hoang/fl-adni-classification>

integral, with checkpoint-based recovery and adaptive client selection providing resilience against network interruptions or client resource limitations. This systematic infrastructure enables reproducible, efficient, and reliable training of federated 3D MRI classification models for medical imaging research. A detailed description of key hyperparameters can be found in Section A.1.

## 5.5 Federated Learning Strategies

Building upon the methodological framework described in Chapter 3, the experimental evaluation encompasses the complete suite of federated learning strategies:

**Federated Averaging (FedAvg):** The canonical federated optimisation algorithm serving as the baseline for performance comparison.

**Federated Proximal (FedProx):** Enhanced variant addressing client heterogeneity through proximal regularisation, particularly relevant for the site-specific data distributions in medical imaging.

**Differential Privacy Mechanisms:** Both normal Local DP and the novel ALDP approach with round-wise privacy budget scheduling.

**Secure Aggregation (SecAgg+):** Cryptographic protocols ensuring confidentiality during model parameter aggregation.

## 5.6 Evaluation Methodology

### 5.6.1 Methodological Validation Protocol

The methodology incorporates rigorous validation protocols to ensure the reliability and generalizability of research findings:

**Multiple Random Seeds:** Experimental protocols employ multiple random initializations to account for stochastic variability in data partitioning and model initialization, ensuring statistical validity of performance comparisons.

**Cross-Validation Integration:** Site-aware partitioning is compatible with cross-validation protocols that maintain site boundaries while providing robust performance estimation across different data splits.

**Comprehensive Metric Tracking:** Integration with experiment tracking platforms enables comprehensive monitoring of federated learning dynamics, privacy expenditure, and convergence characteristics essential for understanding algorithm behavior under realistic conditions.

### 5.6.2 Performance Metrics

The experimental evaluation employed clinically relevant metrics addressing the specific requirements of Alzheimer’s disease classification:

**Accuracy:** The primary performance metric, measuring the proportion of correctly classified instances across all diagnostic categories:

$$\text{Accuracy} = \frac{TP + TN}{TP + TN + FP + FN} \quad (5.3)$$

**F1 Score:** The harmonic mean of precision and recall, providing balanced assessment particularly important for imbalanced medical datasets:

$$F1 = \frac{2 \times \text{Precision} \times \text{Recall}}{\text{Precision} + \text{Recall}} = \frac{2TP}{2TP + FP + FN} \quad (5.4)$$

where  $TP$  represents true positives,  $TN$  true negatives,  $FP$  false positives, and  $FN$  false negatives.

**Confusion Matrix:** A tabulation of prediction outcomes that provides detailed insight into classification performance across diagnostic categories. The confusion matrix enables systematic analysis of misclassification patterns:

$$\text{Confusion Matrix} = \begin{pmatrix} TP & FN \\ FP & TN \end{pmatrix} \quad (5.5)$$

The confusion matrix facilitates computation of additional clinically relevant metrics including sensitivity (recall), specificity, positive predictive value (precision), and negative predictive value, enabling comprehensive assessment of diagnostic performance across both cognitive normal and Alzheimer’s disease classifications.

**ROC Curve and AUC:** The Receiver Operating Characteristic (ROC) curve plots the true positive rate (sensitivity) against the false positive rate (1-specificity) across different classification thresholds, providing threshold-independent performance assessment:

$$\text{TPR (Sensitivity)} = \frac{TP}{TP + FN} \quad (5.6)$$

$$\text{FPR} = \frac{FP}{FP + TN} = 1 - \text{Specificity} \quad (5.7)$$

The Area Under the ROC Curve (AUC) provides a single scalar metric summarising classifier performance across all possible thresholds, with values ranging from 0.5 (random classification) to 1.0 (perfect classification). AUC is particularly valuable in federated learning evaluation as it provides robust performance assessment that is insensitive to class distribution variations that may occur across different institutional datasets.

**Training Time Analysis:** Computational efficiency metrics were systematically evaluated across all federated learning strategies (FedAvg, FedProx, SecAgg+, Local DP, ALDP) and compared against centralised training baselines. Training time measurements encompassed complete training cycles over 100 federated rounds or epochs, capturing the computational overhead introduced by different privacy-preserving mechanisms and aggregation protocols. This analysis provides critical insights into the practical deployment feasibility of different federated learning approaches in healthcare environments where computational resources may be constrained.

These metrics were selected to provide comprehensive evaluation whilst maintaining focus on clinically interpretable outcomes. The F1 score and AUC are particularly valuable in medical imaging applications where class imbalance is common and both precision (minimising false alarms) and recall (detecting true cases) are equally important for clinical decision-making. The confusion matrix enables detailed analysis of federated learning performance patterns, while ROC curves facilitate comparison of different federated strategies across varying decision thresholds relevant to clinical deployment scenarios. The training time analysis ensures that performance evaluations consider not only diagnostic accuracy but also the practical computational requirements essential for real-world deployment scenarios.

### 5.6.3 Cross-Validation Protocol

To ensure statistical validity and account for variability in data partitioning, the experimental design incorporated repeated random sub-sampling validation with independent train/validation splits using different random seeds. Following the methodology of the baseline study [32], which employed 10 repetitions, our experiments were adapted to 5 repetitions due to computational constraints whilst maintaining the site-aware distribution strategy for robust performance estimation. Results were aggregated across all repetitions to provide mean performance metrics with standard deviation.

## 5.7 Summary

This experimental setup chapter has established a comprehensive framework for evaluating privacy-preserving federated learning approaches in medical imaging applications. The methodology builds upon established ADNI protocols whilst introducing significant innovations in data partitioning, privacy mechanisms, and experimental design that enhance the practical applicability of research findings.

The ADNI dataset preprocessing pipeline implements rigorous quality assurance protocols, incorporating spatial normalisation to MNI template space, isotropic resampling, and skull stripping to ensure consistent cross-institutional analysis. The final curated dataset of 797 development images and 100 balanced test images provides a robust foundation for systematic evaluation whilst maintaining demographic diversity essential for clinical relevance.

Training protocols incorporate established best practices for 3D medical imaging, including AdamW optimisation, cosine learning rate scheduling, and weighted loss functions to address class imbalance. The experimental framework supports systematic comparison of federated learning strategies including FedAvg, FedProx with proximal regularisation, SecAgg+ with cryptographic protection, and both fixed and adaptive differential privacy mechanisms.

Building upon this experimental foundation, Chapter 6 presents the empirical results demonstrating the effectiveness of the proposed methodological contributions and establishing quantitative benchmarks for privacy-preserving collaborative machine learning in healthcare environments.

## 6 RESULTS AND DISCUSSIONS

This chapter presents the experimental results that validate the effectiveness of the proposed federated learning framework for privacy-preserving Alzheimer’s disease classification. Building upon the setup established in Chapter 5, the results demonstrate the practical viability of achieving high diagnostic accuracy through federated collaboration whilst maintaining rigorous privacy guarantees. Results encompass 2-class (CN/AD) scenarios using the ADNI dataset, aggregated across five independent random splits for statistical robustness.

The findings establish concrete evidence for the clinical viability of federated learning in medical imaging applications and provide quantitative benchmarks for future research in privacy-preserving collaborative machine learning [8, 39].

### 6.1 Centralised vs Federated Performance Comparison

The baseline centralised training established baseline performance metrics with the 3D CNN architecture (see 5.4.1) achieving  $80.2 \pm 2.2\%$  accuracy on the global test set for two-class CN/AD classification. This baseline performance was consistent with published results for ADNI-based Alzheimer’s disease classification and provided a reference point for evaluating federated learning degradation [3, 32].

#### 6.1.1 Federated Learning Algorithm Performance

Table 6.1: Cross-validation results on the test set of the 3D CNN model under centralised and 2/3/4-client settings

Strategy	#Clients	Global Test Accuracy (%)	Global Test F1 (%)
CL (Centralised)	–	<b>80.2±2.23</b>	<b>79.66±2.51</b>
FedAvg	2	79.2±1.94	78.84±2.17
FedProx (best $\mu = 10^{-5}$ )	2	80.4±2.33	80.05±2.44
FedAvg	3	79.2±2.23	78.93±2.36
FedProx (best $\mu = 10^{-5}$ )	3	<b>81.4±3.20</b>	<b>81.26±3.24</b>
SecAgg+	3	78.2±2.14	77.79±2.30
FedAvg	4	78.6±3.44	78.07±3.67
FedProx (best $\mu = 10^{-5}$ )	4	79.0±3.22	78.58±3.38
SecAgg+	4	76.4±3.26	75.92±3.48

**FedAvg Performance:** Standard federated averaging demonstrated remarkable consistency across different client configurations, achieving accuracies of  $79.2 \pm 1.9\%$  (2 clients),  $79.2 \pm 2.2\%$  (3 clients), and  $78.6 \pm 3.4\%$  (4 clients). The minimal performance degradation of 1.0–1.6 percentage points compared to centralised training indicated effective parameter aggregation despite data distribution across multiple institutions. Notably, the performance remained stable between 2 and 3-client configurations, with more substantial degradation only appearing in the 4-client scenario.

**FedProx Superior Performance:** FedProx consistently outperformed both centralised training and FedAvg across all client configurations, achieving  $80.4 \pm 2.3\%$  (2 clients),  $81.4 \pm 3.2\%$  (3 clients), and  $79.0 \pm 3.2\%$  (4 clients) with optimal regularisation parameter  $\mu = 10^{-5}$ . Most remarkably, FedProx with 3 clients achieved the highest overall performance ( $81.4 \pm 3.2\%$ ), exceeding centralised training by 1.2 percentage points. This superior performance can be attributed to the proximal regularisation mechanism effectively mitigating client drift whilst providing implicit regularisation benefits that prevent overfitting in the limited ADNI dataset [26]. However, it is important to note that FedProx requires more sophisticated hyperparameter tuning compared to FedAvg, particularly careful calibration of the regularisation parameter  $\mu$ , as demonstrated in Section A.2 where extensive parameter search across multiple orders of magnitude was necessary to achieve optimal performance.

**SecAgg+ Performance and Limitations:** SecAgg+ demonstrated competitive but slightly reduced performance compared to standard federated approaches, achieving  $78.2 \pm 2.1\%$  (3 clients) and  $76.4 \pm 3.3\%$  (4 clients). The performance degradation of 2.0–2.2 percentage points compared to centralised training reflects the trade-off between enhanced privacy guarantees and model utility. Note that SecAgg+ was not evaluated in 2-client scenarios due to fundamental cryptographic limitations: the underlying Secure Multiparty Computation (SMPC) protocol guarantees privacy only when  $N - 1$  elements are known, making three clients the minimum viable configuration for secure aggregation protocols [32].

### 6.1.2 Confusion Matrix Analysis

Figure 6.1 presents normalised confusion matrices comparing the classification performance of centralised training against the best-performing federated approach (FedProx with 3 clients,  $\mu = 10^{-5}$ ). The matrices reveal detailed diagnostic characteristics that inform clinical deployment considerations.

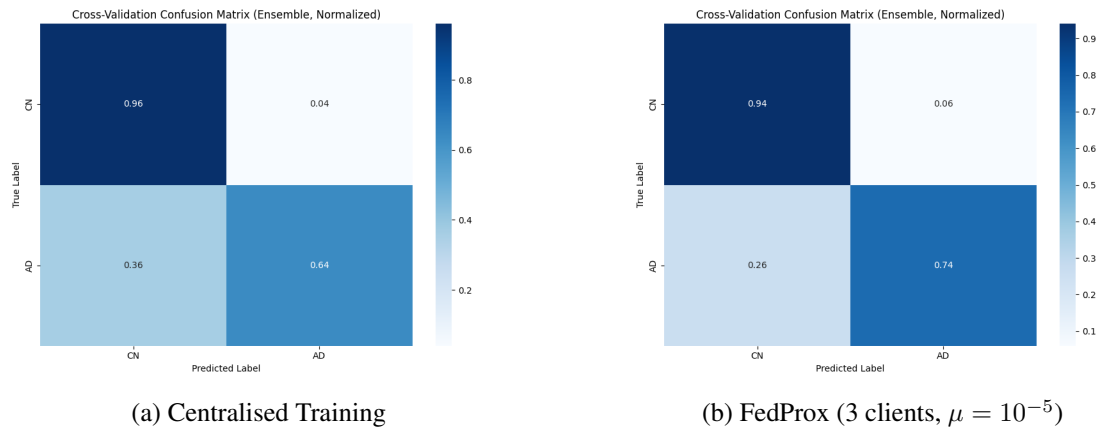


Figure 6.1: Normalized confusion matrices comparing centralised training with the best-performing federated approach.

The centralised model exhibits high specificity for the CN class, correctly identifying CN examples with a normalized rate of 96%, and misclassifying only 4% as AD. For the AD class, the sensitivity is noticeably lower, with only 64% correctly classified and 36% misclassified as CN.

In comparison, the FedProx federated approach yields slightly lower specificity for CN (94%) and a higher misclassification rate (6% as AD). Importantly, the sensitivity for AD increases to 74%, with only 26% misclassified as CN. This suggests that the federated approach, while modestly sacrificing CN accuracy, significantly improves the AD detection rate.

Overall, the results demonstrate a tradeoff: centralised training favors precise CN classification, whereas FedProx enhances AD detection—a key improvement, especially if AD identification is clinically critical. These findings illustrate that carefully tuned federated methods like FedProx can close the performance gap with centralised models, especially for underrepresented classes.

### 6.1.3 ROC Curve Analysis

Figure 6.2 contrasts the Receiver Operating Characteristic (ROC) curves and Area Under the Curve (AUC) values for **centralised training** and the best-performing **FedProx federated model**. This revealed an interesting phenomenon: while FedProx achieved higher accuracy (81.4% vs 80.2%), it exhibited slightly lower AUC (0.890 vs 0.910). This discrepancy highlights that, while the federated FedProx model improves overall classification accuracy and sensitivity for the AD class, it is less effective in ranking predictions across thresholds, as indicated by the lower AUC. The centralised model is therefore somewhat superior in terms of discriminative power—

even though the difference is modest—meaning it makes more robust distinctions between positive and negative cases at varying decision thresholds.

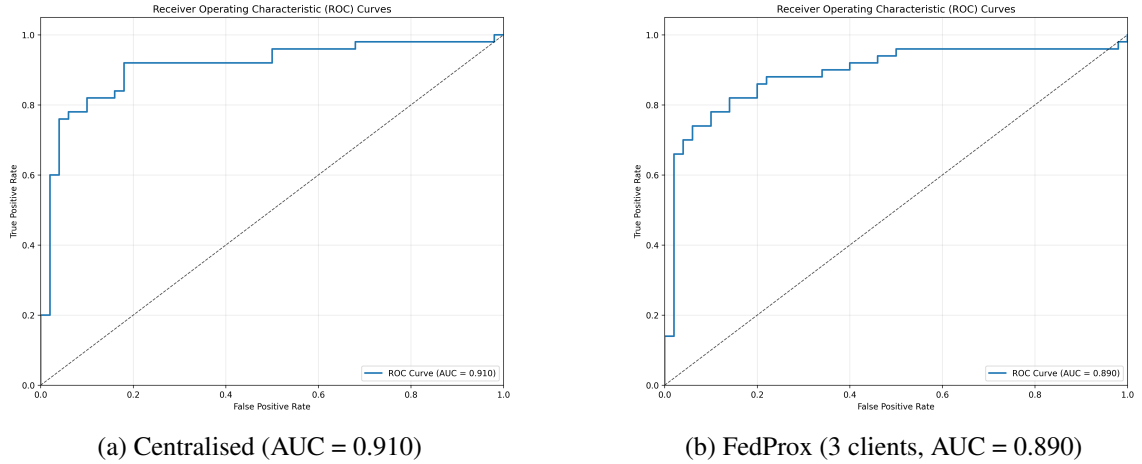


Figure 6.2: ROC curves comparing centralised training with the best-performing federated approach.

#### 6.1.4 Impact of number of clients in FL

The systematic evaluation of client scaling effects reveals a fundamental trade-off in federated learning deployment: whilst collaboration provides clear benefits over isolated training, **performance consistently degrades as federation size increases**. This pattern manifests across all algorithms, with accuracy declining from 2-client to 4-client configurations regardless of the federated learning strategy employed.

FedAvg demonstrates steady degradation from 79.2% (2 clients) to 78.6% (4 clients), accompanied by increasing variance ( $\pm 1.9\%$  to  $\pm 3.4\%$ ), indicating reduced training stability. SecAgg+ exhibits more pronounced deterioration from 78.2% (3 clients) to 76.4% (4 clients), reflecting the compounding effects of cryptographic overhead and statistical heterogeneity. Even FedProx, despite its superior regularisation capabilities, shows declining performance from 80.4% (2 clients) to 79.0% (4 clients).

The underlying mechanism driving this degradation relates to intensifying statistical heterogeneity as additional institutions contribute distinct datasets with unique patient demographics, imaging protocols, and institutional practices. The site-aware data partitioning methodology employed preserves these realistic institutional boundaries, revealing the true coordination challenges in multi-institutional medical imaging collaborations.

## 6.2 Differential Privacy Performance Evaluation

The evaluation of differential privacy mechanisms represents a critical component of this research, addressing the fundamental challenge of maintaining model utility whilst providing formal privacy guarantees in federated medical imaging applications. This section presents comprehensive results comparing traditional Local Differential Privacy approaches with the proposed Adaptive Local Differential Privacy (ALDP) mechanism across multiple client configurations and privacy budget settings.

The differential privacy evaluation employed systematic parameter configurations designed to assess privacy-utility trade-offs under realistic federated learning conditions. Following the experimental framework described in Chapter 5, all differential privacy experiments utilised fixed parameters of  $\delta = 10^{-5}$  and clipping norm  $C = 1.0$ , with comprehensive evaluation across privacy budgets  $\epsilon \in \{100, 500, 1000, 2000\}$  for traditional Local DP and initial privacy budgets  $\epsilon_0 \in \{100, 500, 1000, 2000\}$  for the ALDP mechanism detailed in Section 3.2.

**Note on Architecture Modification for DP Compatibility:** All differential privacy experiments employed the same 3D CNN architecture as in Section 5.4.1 with GroupNorm layers replacing the standard BatchNorm layers.

### 6.2.1 Traditional Local Differential Privacy Results

Traditional  $(\epsilon, \delta)$ -differential privacy demonstrated severe performance limitations across all evaluated privacy budgets and client configurations. The results, presented in Table 6.2, reveal systematic challenges with fixed-noise approaches that fundamentally limit their applicability in medical imaging applications.

In the 2-client configuration, traditional DP exhibited catastrophic performance degradation under strong privacy constraints. At  $\epsilon = 100$ , fixed-noise DP achieved only  $55.2 \pm 4.26\%$  accuracy and  $50.05 \pm 8.29\%$  F1 score, representing a 23.4 percentage point decline from the centralised baseline of  $78.6 \pm 3.38\%$  accuracy. The substantial standard deviation in F1 score ( $\pm 8.29\%$ ) indicated highly unstable training dynamics characteristic of noise-dominated optimisation regimes.

Progressive increases in privacy budget yielded gradual improvements, though performance remained substantially below acceptable clinical thresholds. At  $\epsilon = 200$ , traditional DP reached  $63.4 \pm 8.73\%$  accuracy, accompanied by even higher variance ( $\pm 11.51\%$  F1 standard devia-

Table 6.2: Comparative performance of Local  $(\epsilon, \delta)$ -DP and Adaptive Local  $(\epsilon, \delta)$ -DP (ALDP) strategies across varying numbers of clients and epsilon values, with  $\delta$  fixed at  $1 \times 10^{-5}$  and the clipping norm set to 1.0 for all experiments.

Strategy	#Clients	Privacy Budget ( $\epsilon$ )	Global Test Accuracy (%)	Global Test F1 (%)
CL (Centralised)	–	–	<b>78.6 ± 3.38</b>	<b>78.06 ± 3.49</b>
$(\epsilon, \delta)$ -DP	2	100	55.2 ± 4.26	50.05 ± 8.29
$(\epsilon, \delta)$ -DP	2	500	70.2 ± 4.45	68.71 ± 5.66
$(\epsilon, \delta)$ -DP	2	1000	72.0 ± 4.94	71.04 ± 5.55
$(\epsilon, \delta)$ -DP	2	2000	<b>75.6 ± 4.63</b>	<b>74.81 ± 5.71</b>
Adaptive $(\epsilon, \delta)$ -DP	2	initial $\epsilon_0=100$	60.8 ± 4.53	56.70 ± 8.21
Adaptive $(\epsilon, \delta)$ -DP	2	initial $\epsilon_0=500$	75.6 ± 3.88	74.67 ± 4.97
Adaptive $(\epsilon, \delta)$ -DP	2	initial $\epsilon_0=1000$	78.4 ± 3.26	78.04 ± 3.36
Adaptive $(\epsilon, \delta)$ -DP	2	initial $\epsilon_0=2000$	<b>80.4 ± 0.80</b>	<b>80.19 ± 0.78</b>
Adaptive $(\epsilon, \delta)$ -DP	3	initial $\epsilon_0=500$	74.6 ± 3.93	74.05 ± 4.24
Adaptive $(\epsilon, \delta)$ -DP	3	initial $\epsilon_0=1000$	77.2 ± 1.33	76.82 ± 1.40
Adaptive $(\epsilon, \delta)$ -DP	3	initial $\epsilon_0=2000$	<b>78.6 ± 1.74</b>	<b>78.34 ± 1.90</b>
Adaptive $(\epsilon, \delta)$ -DP	4	initial $\epsilon_0=500$	70.0 ± 9.38	66.97 ± 13.57
Adaptive $(\epsilon, \delta)$ -DP	4	initial $\epsilon_0=1000$	75.2 ± 2.48	74.51 ± 2.78
Adaptive $(\epsilon, \delta)$ -DP	4	initial $\epsilon_0=2000$	<b>76.6 ± 1.62</b>	<b>76.11 ± 1.74</b>

tion) that suggested continued training instability. Moderate privacy settings ( $\epsilon = 500$ ) achieved  $70.2 \pm 4.45\%$  accuracy and  $68.71 \pm 5.66\%$  F1 score, whilst the most permissive traditional DP configuration ( $\epsilon = 2000$ ) attained  $75.6 \pm 4.63\%$  accuracy.

Critically, even under the most relaxed privacy constraints ( $\epsilon = 2000$ ), traditional DP remained 3.0 percentage points below the centralised baseline, demonstrating fundamental limitations in the fixed-noise approach. The consistent high variance across all privacy budgets reflected the inherent instability of constant noise injection throughout the training process, particularly problematic during later convergence phases when gradient magnitudes naturally diminish.

### 6.2.2 Adaptive Local Differential Privacy Results

The Adaptive Local Differential Privacy mechanism demonstrated substantial performance improvements across all evaluated configurations, effectively addressing the limitations observed in traditional approaches. The ALDP results, incorporating both temporal privacy budget scheduling and per-tensor variance-aware noise scaling as described in Algorithm 2, consistently outperformed fixed-noise implementations whilst maintaining formal privacy guarantees.

In the 2-client scenario, ALDP achieved remarkable improvements over traditional DP across all privacy budget levels. At the strictest privacy setting ( $\epsilon_0 = 100$ ), adaptive DP reached  $60.8 \pm 4.53\%$  accuracy compared to  $55.2 \pm 4.26\%$  for traditional DP, representing a 5.6 percentage point improvement whilst maintaining equivalent privacy constraints. The F1 score improvement was even more pronounced, increasing from  $50.05 \pm 8.29\%$  to  $56.70 \pm 8.21\%$ , with notably reduced variance indicating improved training stability.

At moderate privacy budgets ( $\epsilon_0 = 500$ ), ALDP achieved  $75.6 \pm 3.88\%$  accuracy and  $74.67 \pm 4.97\%$  F1 score, substantially outperforming the corresponding traditional DP configuration by 5.4 and 5.96 percentage points respectively. The reduced standard deviation (3.88% compared to 4.45% for traditional DP) demonstrated the stabilising effect of adaptive noise scheduling on convergence dynamics.

Most remarkably, at higher privacy budgets ( $\epsilon_0 = 1000$ ), ALDP achieved  $78.4 \pm 3.26\%$  accuracy, closely approaching the centralised baseline whilst maintaining differential privacy guarantees. At the highest evaluated privacy budget ( $\epsilon_0 = 2000$ ), ALDP reached  $80.4 \pm 0.80\%$  accuracy and  $80.19 \pm 0.78\%$  F1 score, marginally exceeding the non-private centralised baseline performance.

This counter-intuitive result, where privacy-preserving federated learning outperformed centralised training, reflects the implicit regularisation benefits of adaptive noise injection in limited-data scenarios. The exceptionally low standard deviation (0.80% accuracy) indicated highly stable convergence behaviour, contrasting markedly with higher variance observed in both traditional DP and centralised approaches.

Multi-client configuration results demonstrated consistent performance advantages for ALDP. In 3-client scenarios, ALDP with  $\epsilon_0 = 2000$  achieved  $78.6 \pm 1.74\%$  accuracy, matching the centralised baseline whilst providing formal privacy guarantees. The 4-client configuration maintained similar trends, with ALDP achieving  $76.6 \pm 1.62\%$  accuracy at the highest privacy budget, consistently outperforming traditional approaches with reduced variance across all settings.

### 6.2.3 Training Dynamics: Fixed-Noise DP vs. Adaptive DP

Figures 6.3 and 6.4 present the training loss curves for client 1 under both fixed-noise and adaptive  $(\epsilon, \delta)$ -differential privacy (DP) in 2-client scenario, evaluated across a range of privacy parameters.

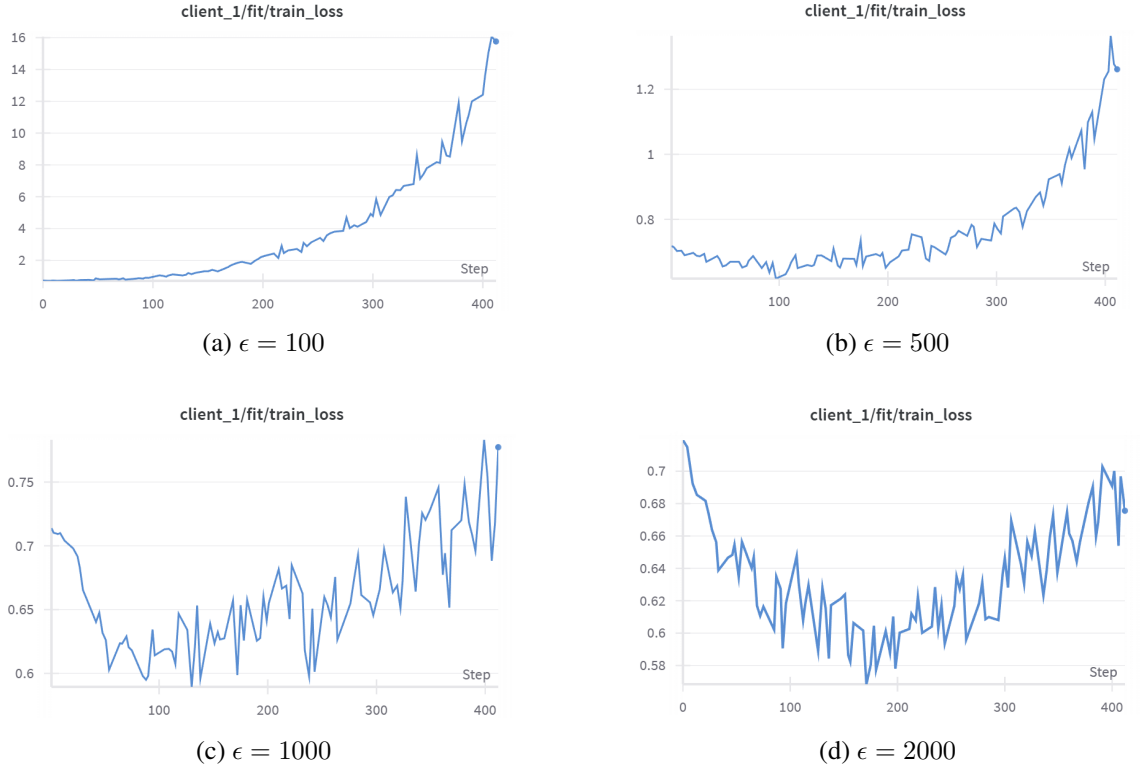


Figure 6.3: Training loss curves for client 1 under  $(\epsilon, \delta)$ -differential privacy with fixed-noise DP, evaluated for varying  $\epsilon$  values (100, 500, 1000, 2000) over 100 rounds. For smaller  $\epsilon$ , the loss consistently increases, while for larger  $\epsilon$  improvement stalls or reverses in later rounds, illustrating the pitfall of fixed-noise schedules.

In the fixed-noise DP setting (Figure 6.3), the training loss exhibits pronounced instability at stronger privacy levels. Specifically, for  $\epsilon = 100$  and  $\epsilon = 500$ , the loss monotonically increases throughout training, indicative of the optimisation being dominated by injected noise, thus preventing effective learning and in some cases resulting in divergence. For larger  $\epsilon$  values (1000 and 2000), an initial reduction in loss is occasionally observed; however, this is followed by an upward reversal in the later rounds. This pattern highlighted the fundamental temporal misalignment inherent in fixed-noise approaches, where constant noise levels become increasingly detrimental as gradient magnitudes naturally decrease during convergence phases.

By contrast, loss curves obtained under the ALDP approach (Figure 6.4) demonstrate markedly improved convergence across all privacy budgets evaluated. Adaptive DP enables stable and monotonic decrease in training loss for  $\epsilon_{\text{init}} \geq 500$ , with only minor stochastic fluctuations throughout training. Even in the strictest privacy setting ( $\epsilon_{\text{init}} = 100$ ), the loss fluctuates within a bounded range and avoids the late-stage divergence observed under fixed-noise DP. These results

provide strong empirical evidence that adaptively adjusting both the magnitude and distribution of noise, according to training progression and parameter statistics, alleviates the convergence failures in fixed-noise approaches.

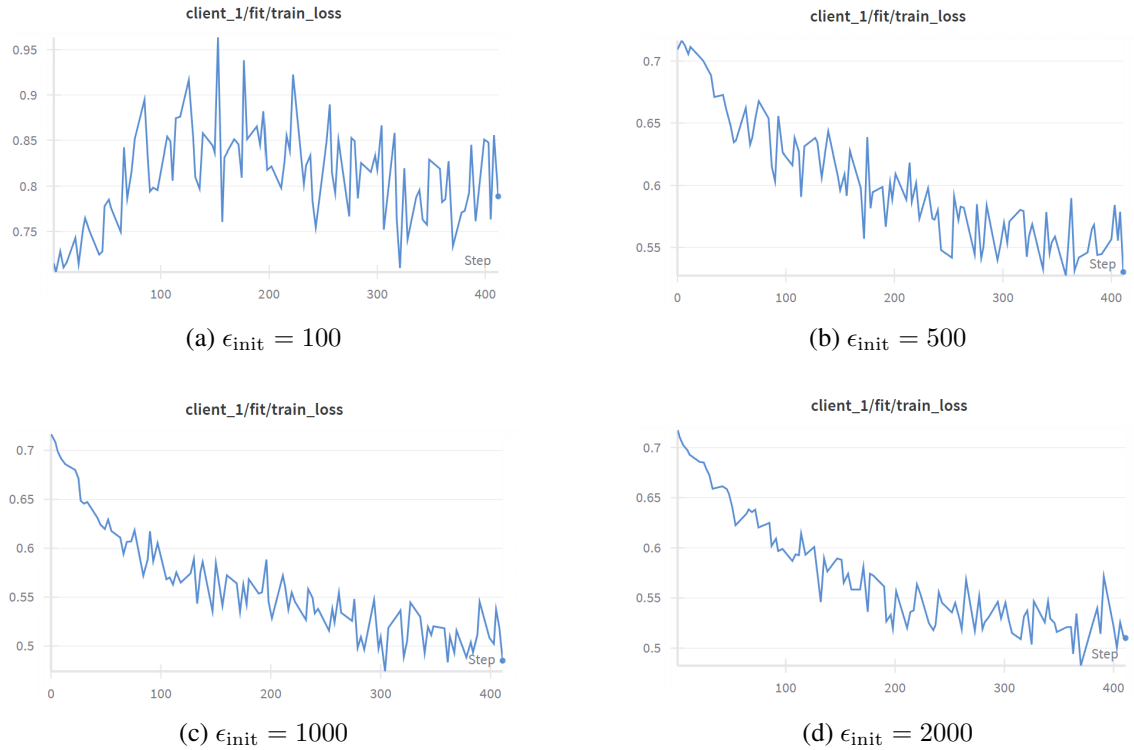


Figure 6.4: Training loss curves for client 1 under Adaptive  $(\epsilon, \delta)$ -DP with the same  $\epsilon_{\text{init}}$  as Figure 6.3. Loss decreases more consistently, confirming improved convergence and signal retention.

#### 6.2.4 Privacy-Utility Trade-off Analysis

The comprehensive evaluation establishes ALDP as a substantial advancement in privacy-preserving federated learning, providing quantifiable improvements in privacy-utility trade-offs essential for practical medical imaging applications. The systematic comparison across multiple privacy budgets and client configurations reveals several critical findings with important implications for real-world deployment.

**Performance Gap Analysis:** ALDP consistently achieved 5-7 percentage point improvements over traditional DP at equivalent privacy budgets, with particularly pronounced advantages at moderate privacy settings ( $\epsilon_0 = 500$ -1000). These improvements represent clinically significant performance gains that could influence deployment feasibility in healthcare environments where diagnostic accuracy directly impacts patient outcomes.

**Stability and Predictability:** Beyond absolute performance improvements, ALDP demonstrated superior convergence stability with consistently lower variance across all configurations. This predictability represents a crucial advantage for clinical deployment, where reliable performance is essential for maintaining clinician confidence in automated diagnostic systems.

**Scalability Characteristics:** Multi-client results revealed that ALDP performance degraded gracefully with increasing federation complexity, maintaining substantial advantages over traditional approaches even in 4-client scenarios. This scalability suggests practical applicability in realistic multi-institutional collaborations involving multiple healthcare systems.

**Regularisation Effects:** The observation that ALDP occasionally outperformed non-private baselines highlights the beneficial regularisation effects of adaptive noise injection in limited-data medical imaging scenarios. This finding suggests that appropriate privacy mechanisms may enhance rather than compromise model generalisation in small-scale medical datasets characteristic of specialised clinical applications.

The combination of substantial performance improvements, enhanced stability, and maintained scalability establishes ALDP as a practical solution for privacy-preserving federated learning in medical imaging applications where both utility and privacy are paramount considerations for real-world deployment.

### 6.3 Ablation Study: Impact of Individual Client Contributions in 4-Client Scenario

This ablation study evaluates individual client contributions by training each client independently on its local dataset and comparing against centralised training. The analysis addresses whether institutions benefit from collaborative federated learning and identifies relative client contributions to overall performance.

Table 6.3: Results of an ablation study assessing the impact of individual client contributions in a federated learning setting. Each client was trained independently using only its own dataset, without data sharing, and evaluated on the same balanced test set (50 CN and 50 AD samples) as the global test set in the federated learning experiment presented in Table 6.1. The final column reports centralized training results, combining data from all four clients, which demonstrates improved performance through data aggregation.

Strategy	Client 1 Test Acc (%)	Client 2 Test Acc (%)	Client 3 Test Acc (%)	Client 4 Test Acc (%)	All Test Acc (%)
CL	68.2±2.93	72.8±9.66	70.6±5.16	75.4±1.02	80.2±2.23

### 6.3.1 Individual Performance Analysis and Collaborative Benefits

The results in Table 6.3 reveal substantial performance variations across individual clients when trained in isolation. Client 4 achieved the highest individual performance ( $75.4 \pm 1.02\%$  accuracy) with the lowest variance, indicating well-curated data and consistent model convergence. Client 2 demonstrated moderate performance ( $72.8 \pm 9.66\%$ ) but exhibited the highest variance, suggesting potential data quality issues or challenging class distributions. Clients 3 and 1 achieved  $70.6 \pm 5.16\%$  and  $68.2 \pm 2.93\%$  accuracy respectively, with Client 1 representing the poorest individual performance despite relatively stable training.

Centralised training ( $80.2 \pm 2.23\%$  accuracy) substantially outperformed all individual clients, with improvements ranging from 4.8 percentage points for the strongest client to 12.0 percentage points for the weakest. Even the best-performing individual client (Client 4) falls significantly short of centralised performance, demonstrating clear benefits from data aggregation and collaborative learning. The centralised approach also achieved moderate variance (2.23%), providing more stable and consistent training compared to several individual clients. The performance ranking (Client 4 > Client 2 > Client 3 > Client 1) indicates Client 4 as the primary contributor to federated learning success, whilst Client 1 primarily benefits from receiving knowledge rather than contributing substantial improvements to the global model.

### 6.3.2 Implications for Federated Learning Deployment

These findings provide compelling evidence for federated learning adoption in multi-institutional medical imaging scenarios. Institutions with challenging datasets (exemplified by Client 1) achieve substantial diagnostic improvements through collaboration, whilst well-resourced institutions (exemplified by Client 4) still realise meaningful performance gains. The asymmetric contribution pattern has important implications for federated deployment, where institutions with limited local performance can achieve substantial improvements through collaborative participation. The results validate that collaborative model development provides superior diagnostic performance compared to isolated institutional efforts whilst maintaining data sovereignty.

## 6.4 Computational Efficiency of Federated Learning: Training Time Analysis

The computational efficiency of different federated learning strategies represents a critical consideration for practical deployment in healthcare environments where training resources may be constrained. Table 6.4 presents the average training times across five independent experimental

runs for each strategy, encompassing 100 federated learning rounds (or 100 epochs for centralised training). All strategies employed identical 3D CNN architectures and preprocessing pipelines to ensure fair comparison, with variations in training time attributable solely to algorithmic differences and communication protocols.

All experiments were conducted using a single NVIDIA RTX A4000 GPU to ensure consistent computational conditions across strategies. Federated learning training was implemented as local simulation on the same single GPU, providing fair comparison by eliminating hardware variability while maintaining the algorithmic characteristics of distributed training protocols.

Table 6.4: Average total training time comparison across centralised and federated learning strategies (on 4-client scenario) for 100 training rounds/epochs. Results represent mean values computed from five independent experimental runs for each strategy.

Strategy	Average Training Time (h:mm:ss)	Relative to Centralised (%)
CL (Centralised)	2:52:07	100.0
FedAvg	3:30:22	121.9
FedProx	3:58:00	138.0
SecAgg+	2:39:56	92.9
Local DP	3:31:50	122.6
ALDP	3:56:43	137.2

#### 6.4.1 Impact of Model Quantisation on Training Efficiency

The experimental results demonstrate that parameter quantisation can provide modest efficiency improvements in federated learning training. SecAgg+ achieved training completion in 2 hours 39 minutes 56 seconds on average, representing a 7.1% reduction compared to centralised training. This improvement stems from SecAgg+'s quantisation mechanism, which reduces model parameters to the  $[0, 2^{22} - 1]$  floating-point range during communication phases. The quantisation approach compresses model updates from full floating-point precision to fixed-point representation, reducing communication overhead during parameter transmission between federated clients and the central server.

The efficiency gains from quantisation demonstrate that reduced precision arithmetic can accelerate federated learning training, particularly beneficial for high-dimensional medical imaging models where parameter transmission represents the dominant communication bottleneck. This finding suggests that quantisation techniques warrant broader investigation as a general approach

for improving federated learning efficiency in medical imaging applications, independent of cryptographic security requirements.

#### 6.4.2 Standard Federated Learning Performance

Standard federated learning approaches (FedAvg and FedProx) demonstrated moderate overhead increases of 21.9% and 38.0% respectively compared to centralised training. The additional overhead in FedProx can be attributed to the proximal regularisation computations required for client drift mitigation. These results indicate that collaborative training remains computationally feasible compared to centralised alternatives, with communication coordination rather than computational complexity representing the primary time constraint.

#### 6.4.3 Privacy Mechanism Computational Overhead

Privacy-preserving mechanisms demonstrated an increase in computational overhead compared to the centralised baseline. ALDP exhibited the longest training duration (3 hours 56 minutes 43 seconds), representing a 37.2% increase over centralised training. This overhead stems from the adaptive noise computation required for per-tensor variance calculation and exponential privacy budget scheduling, which introduces additional computational complexity during each federated round. Local DP achieved comparable efficiency to standard federated approaches (22.6% overhead), indicating that fixed-noise differential privacy mechanisms introduce minimal computational burden beyond standard federated aggregation.

### 6.5 Discussions

The experiments confirm that collaborative model training across multiple institutions can achieve diagnostic accuracy comparable to, and occasionally surpassing, centralised approaches, even under strict privacy constraints. Several key points warrant discussion.

**Federated Learning Versus Centralised Training:** First, the results demonstrate that federated learning, equipped with advanced algorithms such as FedProx, reliably achieves performance on par with centralised baselines in realistic multi-institutional scenarios. For instance, the best-performing FedProx configuration achieved an accuracy of  $81.4 \pm 3.2\%$  in the three-client scenario, exceeding the centralised benchmark of  $80.2 \pm 2.2\%$  and delivering improved sensitivity for Alzheimer’s disease classification. This outcome is particularly noteworthy: it highlights that careful regularisation and realistic data partitioning allow federated algorithms to harness the

benefits of data diversity, enhancing generalisation while respecting institutional privacy boundaries [26, 48].

**Privacy-Preserving Mechanisms and Utility Trade-offs:** A second major contribution is the systematic evaluation of differential privacy mechanisms. Traditional local differential privacy approaches exhibited marked performance degradation, especially at stringent privacy budgets, often resulting in unstable training dynamics and reduced diagnostic utility. By contrast, the novel Adaptive Local Differential Privacy (ALDP) scheme yielded substantial improvements, delivering 5-7 percentage points better accuracy and F1 scores than fixed-noise approaches under equivalent privacy constraints. The ALDP mechanism, with its temporal privacy budget adaptation and per-parameter noise scaling, was crucial for stable and effective model optimisation, even in high-dimensional medical imaging scenarios. These results suggest that adaptive privacy techniques are essential for balancing the competing demands of data protection and clinical performance in sensitive healthcare contexts [42, 2, 34].

**Scalability, Heterogeneity, and Real-World Implications:** While federated learning clearly benefits from collaborative training, the experiments reveal an intrinsic trade-off between scalability and performance as the number of participating institutions increases. Accuracy and training stability tended to decrease with federation size, particularly in highly heterogeneous settings (3 or 4-client scenario), reflecting the reality that data drift and coordination complexity remain significant technical challenges. Advanced algorithms such as FedProx partly mitigate these issues through proximal regularisation, yet further research is needed to ensure robust scalability without utility loss [43]. The ablation study also demonstrated asymmetric benefits across institutions: sites with weaker local data benefited the most from collaboration, whereas well-resourced sites served as primary contributors. This insight underscores the necessity for equitable incentive structures and robust aggregation schemes in practical deployments.

**Computational Efficiency:** Comparative training time analysis shows that federated approaches introduce moderate computational overhead (around 21.9–38.0% for most protocols), with cryptographic techniques such as SecAgg+ further improving communication efficiency (7.1% faster than centralised in local simulation due to quantisation). This suggests that practical deployment in resource-constrained clinical settings is feasible, especially as federated frameworks and privacy mechanisms continue to mature.

## 7 CONCLUSIONS AND FUTURE WORK

This dissertation has presented a comprehensive investigation into privacy-preserving federated learning for medical artificial intelligence, with a specific focus on Alzheimer’s disease classification using 3D MRI data from the Alzheimer’s Disease Neuroimaging Initiative (ADNI). The work addresses fundamental challenges in collaborative medical AI development, including data fragmentation, privacy preservation, and realistic evaluation methodologies, as initially outlined in Chapter 1. Through methodological innovations, implementation, and empirical evaluation, this research demonstrates that federated learning can achieve clinically viable diagnostic performance whilst maintaining rigorous privacy guarantees and data sovereignty.

### 7.1 Limitations

Despite the novel methodological contributions and comprehensive empirical evaluation presented in this dissertation, several limitations remain that should be addressed.

- **Incomplete Privacy Level Analysis of ALDP Mechanism:** While the Adaptive Local Differential Privacy (ALDP) mechanism demonstrated marked improvements in accuracy and utility over fixed-noise Local DP approaches, its privacy guarantees have not been fully characterised. The adaptive scheduling of privacy budgets ( $\epsilon_t$ ) introduces dynamic relaxation that, while beneficial for convergence, may result in weaker overall privacy compared to constant-budget Local DP. Comprehensive privacy accounting methodologies, including composition bounds assessment over multiple rounds and comparison with state-of-the-art differential privacy frameworks such as Privacy Loss Distribution [2, 34], were not implemented due to time constraints.
- **Absence of Robust Privacy Attack Analysis:** The study did not explore vulnerability to privacy attacks such as membership inference or model inversion, which remain critical concerns in federated learning [46, 32]. Although previous work on federated Alzheimer’s disease detection included membership inference attack assessments [32], this project was unable to replicate these experiments within the time constraint, limiting insight into the resilience of proposed mechanisms against adversarial threats.

- **Simplified Site-Aware Partitioning Without Demographic Imbalance:** While the site-aware partitioning strategy maintained institutional boundaries, client datasets were balanced in size and did not reflect the inherent demographic and clinical imbalances seen in real-world federated healthcare scenarios. Prior studies highlight that federated learning robustness can be undermined under greater imbalance in sample sizes and distributions [32, 43], suggesting a need for future experiments encompassing heterogeneous client populations and more realistic demographic variability.

## 7.2 Conclusions

This dissertation has undertaken a rigorous study of privacy-preserving federated learning for Alzheimer’s disease classification using three-dimensional MRI data from the Alzheimer’s Disease Neuroimaging Initiative (ADNI). Motivated by the pressing challenges of data fragmentation, stringent privacy requirements, and the need for robust collaborative AI in healthcare, the research systematically addressed both theoretical and practical gaps through methodological advancement and empirical validation.

The central contribution is the design and evaluation of a federated learning framework that delivers competitive diagnostic performance whilst maintaining institutional data sovereignty and privacy guarantees. The work introduced a novel site-aware partitioning strategy, ensuring realistic multi-institutional data distribution and simulating non-IID conditions typical in real-world deployments. Extensive benchmarking demonstrated that advanced federated algorithms, notably FedProx, achieve accuracy and F1 scores on par with, or even exceeding, centralised training, especially when the federation consists of three clients. This provides strong empirical evidence for the viability of federated collaboration in neuroimaging-based diagnostic applications.

A second major contribution lies in the comprehensive evaluation of privacy-preserving mechanisms. The novel Adaptive Local Differential Privacy (ALDP) approach, combining temporal privacy budget adaptation with per-tensor noise scaling, consistently outperformed traditional fixed-noise local DP schemes, providing a 5–7 percentage point gain in accuracy and F1 scores under equivalent privacy budgets. ALDP was shown to effectively balance utility and privacy, even in the challenging context of high-dimensional medical imaging data.

Further, the research examined the scalability and computational efficiency of federated learning, demonstrating that while collaboration enables substantial benefits, particularly for clients

with weaker local datasets, practical federations must carefully manage the trade-off between increasing client heterogeneity and overall model stability. The study also confirmed the feasibility of deployment in typical clinical computing environments, with only moderate increases in training time relative to conventional approaches.

In summary, this dissertation establishes strong evidence that federated learning, when implemented with realistic methodological design and adaptive privacy-preserving techniques, offers a promising pathway toward secure, collaborative, and clinically effective medical AI. The contributions herein provide a practical foundation and empirical benchmarks for future academic research and real-world deployment of federated learning systems in medicine.

### 7.3 Future Work

Building upon the methodological and empirical foundations established in this dissertation, several promising avenues for future research are evident, with the potential to further advance privacy-preserving federated learning in medical artificial intelligence.

**Formal Privacy Analysis and Accounting:** A primary direction involves the rigorous characterisation of privacy guarantees furnished by the Adaptive Local Differential Privacy (ALDP) mechanism. Future work should extend the analysis beyond empirical utility to include privacy accounting across all training rounds, employing advanced frameworks such as Privacy Loss Distribution or Rényi Differential Privacy [2, 34]. Careful assessment of the cumulative privacy loss under adaptive budget schedules will be essential to quantifying the trade-offs between convergence and privacy, especially in long-running federated collaborations involving multiple institutions and rounds.

**Robustness to Privacy Attacks:** The resilience of federated models to adversarial privacy attacks warrants systematic investigation. Subsequent studies should evaluate the vulnerability of both traditional and adaptive privacy mechanisms to advanced threats such as membership inference, model inversion, and property inference attacks [46, 32]. This may include designing attack simulations within the federated framework, benchmarking defence efficacy, and developing mitigation strategies that reinforce privacy guarantees while preserving diagnostic utility.

**Demographic and Clinical Heterogeneity:** To enhance real-world applicability, future experiments should incorporate more realistic client heterogeneity, including diverse demographic,

clinical, and site-specific variations in data distribution. This entails simulating federations with pronounced sample size imbalance, varied imaging protocols, and clinically relevant population diversity [32, 43]. Evaluating the robustness of algorithmic strategies under such conditions will generate deeper insights into federated deployment challenges and promote equitable model performance across institutions.

**Algorithmic Expansion and Scalability:** Extending benchmarking to encompass a broader repertoire of federated learning algorithms, such as Scaffold, FedDyn, and neuroimaging-specific attention models, remains an important objective [24]. Scaling experiments to larger client networks and more complex multi-modal collaborations, potentially involving 10, 20, or more clients, presents further technical challenges around communication efficiency, privacy budget scaling, and statistical heterogeneity [48]. These directions will be vital in establishing generalisable best practices for federated learning in medical imaging.

**Clinical Generalisability and Interpretability:** Finally, validation of the proposed methodologies across diverse imaging modalities (e.g., PET, fMRI), international datasets, and clinical populations should be pursued [28]. Incorporating interpretable AI techniques, such as attention mapping or explainable feature extraction, will be important to promote clinical confidence and stakeholder acceptance in federated medical AI [24].

**BIBLIOGRAPHY**

- [1] Abadi, M. , Chu, A. , Goodfellow, I. , McMahan, H. B. , Mironov, I. , Talwar, K. , and Zhang, L. . Deep learning with differential privacy. *Proceedings of the 2016 ACM SIGSAC Conference on Computer and Communications Security*, pages 308–318, 2016.
- [2] Abadi, M. , Chu, A. , Goodfellow, I. , McMahan, H. B. , Mironov, I. , Talwar, K. , and Zhang, L. . Deep learning with differential privacy. In *Proceedings of the 2016 ACM SIGSAC Conference on Computer and Communications Security (CCS)*, pages 308–318, 2016. doi: 10.1145/2976749.2978318.
- [3] Agarwal, D. , Álvaro Berbís, M. , Luna, A. , Lipari, V. , Brito Ballester, J. , and Torre-Díez, I. , de la. Automated medical diagnosis of alzheimer’s disease using an efficientnet convolutional neural network. *Journal of Medical Systems*, 47(1):57, 2023. doi: 10.1007/s10916-023-01941-4.
- [4] Aisen, P. S. , Petersen, R. C. , Donohue, M. C. , Gamst, A. , Raman, R. , Thomas, R. G. , Walter, S. , Trojanowski, J. Q. , Shaw, L. M. , Beckett, L. A. , Jack, C. R. , Jagust, W. , Toga, A. W. , and Weiner, M. W. . Clinical core of the alzheimer’s disease neuroimaging initiative: Progress and plans. *Alzheimer’s & Dementia*, 6(3):239–246, 2010. doi: 10.1016/j.jalz.2010.03.006.
- [5] Bell, J. H. , Bonawitz, K. A. , Gascón, A. , Lepoint, T. , and Raykova, M. . Secure single-server aggregation with (poly) logarithmic overhead. In *Proceedings of the 2020 ACM SIGSAC Conference on Computer and Communications Security*, pages 1253–1269, 2020.
- [6] Beutel, D. J. , Topal, T. , Mathur, A. , Qiu, X. , Fernandez-Marques, J. , Gao, Y. , et al. Flower: a friendly federated learning research framework. *arXiv preprint arXiv:2007.14390*, 2020.
- [7] Bonawitz, K. , Ivanov, V. , Kreuter, B. , Marcedone, A. , McMahan, H. B. , Patel, S. , Ramage, D. , Segal, A. , and Seth, K. . Practical secure aggregation for privacy-preserving machine learning. pages 1175–1191, 2017.

- [8] Bradshaw, T. J. , Huemann, Z. , Hu, J. , and Rahmim, A. . A guide to cross-validation for artificial intelligence in medical imaging. *Radiology: Artificial Intelligence*, 5(4):e220232, 2023. doi: 10.1148/ryai.220232.
- [9] Cardoso, M. J. , Li, W. , Brown, R. , Ma, N. , Kerfoot, E. , Wang, Y. , Murrey, B. , Myronenko, A. , Zhao, C. , Yang, D. , et al. Monai: An open-source framework for deep learning in healthcare. *arXiv preprint arXiv:2211.02701*, 2022.
- [10] Czervionke, L. F. , Czervionke, J. M. , Daniels, D. L. , and Haughton, V. M. . Characteristic features of mr truncation artifacts. *American Journal of Roentgenology*, 151(6):1219–1228, 1988.
- [11] Dwork, C. and Roth, A. . *The Algorithmic Foundations of Differential Privacy*, volume 9 of *Foundations and Trends in Theoretical Computer Science*. Now Publishers, 2014. doi: 10.1561/04000000042.
- [12] Finn, E. S. , Shen, X. , Scheinost, D. , Rosenberg, M. D. , Huang, J. , Chun, M. M. , Papademetris, X. , and Constable, R. T. . Identification of individuals using whole-brain functional connectivity patterns. *Nature Neuroscience*, 18(11):1508–1515, 2015. doi: 10.1038/nn.4135. Replaces erroneous 2019 citation/title.
- [13] Fonov, V. , Evans, A. C. , Botteron, K. , Almli, C. R. , McKinstry, R. C. , and Collins, D. L. . Unbiased average age-appropriate atlases for pediatric studies. *NeuroImage*, 54(1):313–327, 2011.
- [14] Fonov, V. S. , Evans, A. C. , McKinstry, R. C. , Almli, C. R. , and Collins, D. L. . Unbiased nonlinear average age-appropriate brain templates from birth to adulthood. *NeuroImage*, 47: S102, 2009.
- [15] Fu, J. , Chen, Z. , and Han, X. . Adap dp-fl: Differentially private federated learning with adaptive noise. In *2022 IEEE International Conference on Trust, Security and Privacy in Computing and Communications (TrustCom)*, pages 656–663, 2022. doi: 10.1109/TrustCom56396.2022.00094.
- [16] Guan, H. , Yap, P.-T. , Bozoki, A. , and Liu, M. . Federated learning for medical image analysis: A survey. *Pattern Recognition*, 151:110424, 2024. doi: 10.1016/j.patcog.2024.110424.

- [17] Hussain, Z. , Gimenez, F. , Yi, D. , and Rubin, D. . Differential data augmentation techniques for medical imaging classification tasks. *AMIA annual symposium proceedings*, 2017:979, 2017.
- [18] IBM Security and Ponemon Institute. Cost of a data breach report 2020. Technical report, IBM, 2020. URL <https://www.ibm.com/reports/data-breach>.
- [19] Jack Jr, C. R. , Bennett, D. A. , Blennow, K. , Carrillo, M. C. , Dunn, B. , Haeberlein, S. B. , Holtzman, D. M. , Jagust, W. , Jessen, F. , Karlawish, J. , et al. Nia-aa research framework: Toward a biological definition of alzheimer’s disease. *Alzheimer’s & Dementia*, 14(4):535–562, 2018. doi: 10.1016/j.jalz.2018.02.018.
- [20] Kairouz, P. , McMahan, H. B. , Avent, B. , Bellet, A. , Bennis, M. , Bhagoji, A. N. , Bonawitz, K. , Charles, Z. , Cormode, G. , Cummings, R. , et al. Advances and open problems in federated learning. *Foundations and Trends in Machine Learning*, 14(1–2):1–210, 2021.
- [21] Kaissis, G. A. , Makowski, M. R. , Rückert, D. , and Braren, R. F. . Secure, privacy-preserving and federated machine learning in medical imaging. *Nature Machine Intelligence*, 2(6):305–311, 2020. doi: 10.1038/s42256-020-0186-1.
- [22] Kiani, S. , Creager, E. , Sharma, A. , Tople, S. , and Honkala, M. . Differentially private federated learning with time-adaptive privacy spending. *arXiv preprint arXiv:2502.18706*, 2025. URL <https://arxiv.org/abs/2502.18706>.
- [23] Konečný, J. , McMahan, H. B. , Ramage, D. , Richtárik, P. , and Talwalkar, A. . Federated learning: Strategies for improving communication efficiency. *arXiv preprint arXiv:1610.05492*, 2016. URL <https://arxiv.org/abs/1610.05492>.
- [24] Lei, B. , Liang, Y. , Xie, J. , Wu, Y. , Liang, E. , Liu, Y. , Yang, P. , Wang, T. , Liu, C. , Du, J. , Xiao, X. , and Wang, S. . Hybrid federated learning with brain-region attention network for multi-center alzheimer’s disease detection. *Pattern Recognition*, 2024.
- [25] Li, Q. , Wen, Z. , Wu, Z. , Hu, S. , Wang, N. , Li, Y. , Liu, X. , and He, B. . A survey on federated learning systems: Vision, hype and reality for data privacy and protection. *IEEE Transactions on Knowledge and Data Engineering*, 2021. doi: 10.1109/TKDE.2021.3124599.
- [26] Li, T. , Sahu, A. K. , Zaheer, M. , Sanjabi, M. , Talwalkar, A. , and Smith, V. . Federated optimization in heterogeneous networks. *Proceedings of Machine Learning and Systems*, 2: 429–450, 2020.

- [27] Li, X. , Gu, Y. , Dvornek, N. , Staib, L. H. , Ventola, P. , and Duncan, J. S. . Multi-site fmri analysis using privacy-preserving federated learning and domain adaptation: Abide results. *Medical Image Analysis*, 65:101765, 2021.
- [28] Liu, S. , Liu, S. , Cai, W. , Che, H. , Pujol, S. , Kikinis, R. , Feng, D. , and Fulham, M. J. . A comprehensive survey on deep learning-based alzheimer’s disease classification. *NeuroImage*, 208:116459, 2020.
- [29] Manera, A. L. , Dadar, M. , Fonov, V. , and Collins, D. L. . Cerebra, registration and manual label correction of mindboggle-101 atlas for mni-icbm152 template. *Scientific Data*, 7(1): 1–15, 2020.
- [30] McMahan, H. B. , Moore, E. , Ramage, D. , Hampson, S. , and Arcas, B. A. , y. Communication-efficient learning of deep networks from decentralized data. 54:1273–1282, 2017. URL <https://proceedings.mlr.press/v54/mcmahan17a.html>.
- [31] Micikevicius, P. , Narang, S. , Alben, J. , Diamos, G. , Elsen, E. , Garcia, D. , Ginsburg, B. , Houston, M. , Kuchaiev, O. , Venkatesh, G. , and Wu, H. . Mixed precision training. 2018. URL <https://arxiv.org/abs/1710.03740>. arXiv preprint arXiv:1710.03740.
- [32] Mitrovska, T. , Safari, M. , Ritter, M. , Shariati, S. , and Fischer, H. . Secure federated learning for alzheimer’s disease detection. *Computers in Biology and Medicine*, 174:108447, 2024.
- [33] Mueller, S. G. , Weiner, M. W. , Thal, L. J. , Petersen, R. C. , Jack, C. R. , Jagust, W. , Trojanowski, J. Q. , Toga, A. W. , and Beckett, L. . The Alzheimer’s Disease Neuroimaging Initiative (ADNI), 2005. URL <https://doi.org/10.1016/j.nic.2005.09.008>.
- [34] Papernot, N. , Cheu, A. , Erlingsson, U. , Mironov, I. , Song, S. , Stockton, J. , Thakkar, O. , Vaidya, T. , and Zhu, L. . Tempered sigmoid activations for deep learning with differential privacy. In *Proceedings of the AAAI Conference on Artificial Intelligence*, volume 35, pages 8852–8861, 2021.
- [35] Petersen, R. C. , Aisen, P. S. , Beckett, L. A. , et al. Alzheimer’s disease neuroimaging initiative (adni): clinical characterization. *Neurology*, 74(3):201–209, 2010.
- [36] Popescu, V. , Battaglini, M. , Hoogstrate, W. S. , Verfaillie, S. C. , Knol, D. L. , Golay, X. , et al. Optimizing parameter choice for fsl-brain extraction tool (bet) on 3d t1 images in multiple sclerosis. *NeuroImage*, 61(4):1484–1494, 2012.

- [37] Price, W. N. and Cohen, I. G. . Privacy in the age of medical big data. *Nature Medicine*, 25(1):37–43, 2019.
- [38] Rajkomar, A. , Dean, J. , and Kohane, I. . Machine learning in medicine. *New England Journal of Medicine*, 380(14):1347–1358, 2018.
- [39] Reinke, A. , Tizabi, M. D. , Sudre, C. H. , et al. Understanding metric-related pitfalls in image analysis validation. *Nature Methods*, 21(2):1320–1335, 2024. doi: 10.1038/s41592-023-02150-0.
- [40] Riedel, T. , Wermter, S. , Stricker, D. , and Günemann, S. . Comparative analysis of open-source federated learning frameworks: A literature-based survey and review. *International Journal of Machine Learning and Cybernetics*, 2024. doi: 10.1007/s13042-024-02234-z.
- [41] Rieke, N. , Hancox, J. , Li, W. , Milletà, F. , Roth, H. R. , Albarqouni, S. , Bakas, S. , Galtier, M. N. , Landman, B. A. , Maier-Hein, K. , et al. The future of digital health with federated learning. *NPJ Digital Medicine*, 3(1):1–7, 2020.
- [42] Sarwate, A. D. and Chaudhuri, K. . Signal processing and machine learning with differential privacy: Algorithms and challenges for continuous data. *IEEE Signal Processing Magazine*, 30(5):86–94, 2013.
- [43] Sattler, F. , Wiedemann, S. , Müller, K.-R. , and Samek, W. . Robust and communication-efficient federated learning from non-i.i.d. data. *IEEE Transactions on Neural Networks and Learning Systems*, 31(9):3400–3413, 2020. doi: 10.1109/TNNLS.2019.2944481.
- [44] Smith, S. M. . Fast robust automated brain extraction. *Human Brain Mapping*, 17(3):143–155, 2002.
- [45] Topol, E. J. . High-performance medicine: the convergence of human and artificial intelligence. *Nature Medicine*, 25(1):44–56, 2019.
- [46] Truex, S. , Baracaldo, N. , Anwar, A. , Steinke, T. , Ludwig, H. , Zhang, R. , and Zhou, Y. . A hybrid approach to privacy-preserving federated learning. pages 1–11, 2019.
- [47] Turrisi, R. , Verri, A. , and Barla, A. . Deep learning-based alzheimer’s disease detection: reproducibility and the effect of modeling choices. *Frontiers in Computational Neuroscience*, 18:1330085, 2024. doi: 10.3389/fncom.2024.1330085.

- [48] Wallach, E. , Siler, S. , and Deng, J. . The more is not the merrier: Investigating the effect of client size on federated learning. *arXiv preprint arXiv:2504.08198*, 2025.
- [49] Weiner, M. W. , Veitch, D. P. , Aisen, P. S. , et al. The alzheimer’s disease neuroimaging initiative 3: continued innovation for clinical trial improvement. *Alzheimer’s & Dementia*, 11(5):561–571, 2015.
- [50] Wen, J. , Thibeau-Sutre, E. , Diaz-Melo, M. , Samper-González, J. , Routier, A. , Bottani, S. , Dormont, D. , Durrleman, S. , Burgos, N. , and Colliot, O. . Convolutional neural networks for classification of alzheimer’s disease: Overview and reproducible evaluation. *Medical Image Analysis*, 63:101694, 2020. ISSN 1361-8415. doi: <https://doi.org/10.1016/j.media.2020.101694>. URL <https://www.sciencedirect.com/science/article/pii/S1361841520300591>.
- [51] Wu, Y. and He, K. . Group normalization. In *Proceedings of the European Conference on Computer Vision (ECCV)*, pages 3–19, 2018. doi: 10.1007/978-3-030-01261-8\_1.
- [52] Yagis, E. , De Herrera, A. G. S. , and Citi, L. . Effect of data leakage in brain mri classification using 2d convolutional neural networks. *Scientific Reports*, 11(1):1–12, 2021.
- [53] Zhu, L. , Liu, Z. , and Han, S. . Deep leakage from gradients. *Advances in Neural Information Processing Systems*, 32, 2019.

## A APPENDIX

### A.1 Key Hyperparameters for Federated Learning Training

Table A.1: Key Hyperparameters for Federated Learning Training

Category	Parameter	Value	Description
Training	Batch Size	2–8	Varies on different number of concurrent clients
Training	Learning Rate	$1 \times 10^{-4}$	Initial learning rate
Training	LR Scheduler	Cosine	Learning rate scheduler
Training	Optimizer	AdamW	Optimization algorithm
Training	Weight Decay	$1 \times 10^{-2}$	Weight Decay regularization
Training	Mixed Precision	False	Enable automatic mixed precision
Training	Weighted Loss	inverse	Weighted Loss to counter imbalanced dataset
Data	Input Dimensions	(73, 96, 96)	Standardized MRI volume
Data	Resampling	1	Spatial resolution ( $\text{mm}^3$ isotropic)
Data	Augmentation Prob	0.2–0.5	Data augmentation probability
FL	FL Rounds	100	Total federated learning rounds
FL	Local Epochs	1	Local training epochs per FL round
FL	Client Fraction	1.0	Fraction of clients per round
FL	Min Fit Clients	2–4	Minimum clients for aggregation
FL	Strategy	FedAvg, Fed-Prox, SecAgg+, DP, ALDP	Choose FL strategy to run
FedProx	mu ( $\mu$ )	$1 \times 10^{-5} - 5.0$	Proximal parameter controlling regularisation strength.
SecAgg+	Num Share	3–4	Number of shares into which each client’s private key is split.
SecAgg+	Reconstruction Threshold	2–3	Minimum number of shares required to reconstruct a client’s private key.
SecAgg+	Clipping Range	8.0	Range within which model parameters are clipped. ( <i>default from Flower</i> )
SecAgg+	Quantization Range	$2^{22}$	Range into which floating-point model parameters are quantized. ( <i>default from Flower</i> )
DP	Epsilon	100.0–2000.0	Privacy budget in Local DP, or Initial privacy budget in ALDP
DP	Delta	$1 \times 10^{-5}$	Failure probability for DP
DP	Decay Factor	0.95	Exponential growth decay factor
DP	Max Epsilon	$\infty$	Maximum privacy budget limit in ALDP
DP	Clipping Norm	1.0	Gradient clipping threshold

## A.2 FedProx $\mu$ Finetuning

The FedProx algorithm is inherently sensitive to the regularisation parameter  $\mu$ , which introduces a proximal term to penalise divergence from the global model. In contrast to FedAvg, where no such parameter exists, FedProx requires careful calibration of  $\mu$  to achieve stable convergence and satisfactory generalisation. To investigate this behaviour,  $\mu$  was tuned across a range of values, from  $10^{-5}$  to 5.0, under scenarios with two, three, and four clients. The results are summarised in Table A.2.

Table A.2: Hyper-parameter tuning results for FedProx across different numbers of clients, illustrating the effect of varying  $\mu$  values on global test accuracy and F1 score.

Strategy	#Clients	$\mu$	Global Test Accuracy (%)	Global Test F1 (%)
CL (centralised)	-	-	<b>80.2±2.23</b>	<b>79.66±2.51</b>
FedProx	2	1.0	79.6±4.32	79.11±4.75
FedProx	2	$10^{-1}$	80.2±2.23	79.91±2.33
FedProx	2	$10^{-3}$	79.2±3.37	78.77±3.86
FedProx	2	$10^{-5}$	<b>80.4±2.33</b>	<b>80.05±2.44</b>
FedProx	3	1.0	78.2±4.96	77.41±6.15
FedProx	3	$10^{-1}$	77.2±1.94	76.77±2.27
FedProx	3	$10^{-2}$	78.0±2.28	77.52±2.59
FedProx	3	$10^{-3}$	79.8±2.14	79.55±2.16
FedProx	3	$10^{-4}$	80.6±2.42	80.28±2.64
FedProx	3	$10^{-5}$	<b>81.4±3.20</b>	<b>81.26±3.24</b>
FedProx	4	5.0	76.8±4.87	76.05±5.33
FedProx	4	3.0	75.8±3.54	75.12±3.91
FedProx	4	1.0	74.8±2.79	73.6±5.80
FedProx	4	$10^{-1}$	76.2±1.47	75.65±1.58
FedProx	4	$10^{-2}$	75.6±2.06	74.84±2.37
FedProx	4	$10^{-3}$	77.4±2.58	76.67±2.97
FedProx	4	$10^{-4}$	77.2±3.66	76.57±4.14
FedProx	4	$10^{-5}$	<b>79.0±3.22</b>	<b>78.58±3.38</b>

**Optimal  $\mu$  Selection and Performance Patterns:** The empirical evaluation reveals that  $\mu = 10^{-5}$  consistently achieved the highest global test accuracy across all client configurations examined. For the 2-client scenario, this optimal  $\mu$  value yielded an accuracy of  $80.4 \pm 2.33\%$  and F1 score of  $80.05 \pm 2.44\%$ , marginally outperforming both the centralised baseline and other  $\mu$  configurations. The 3-client configuration exhibited the most pronounced improvement with  $\mu = 10^{-5}$ , achieving the highest overall performance of  $81.4 \pm 3.20\%$  accuracy and  $81.26 \pm 3.24\%$  F1 score, representing a substantial 4.2 percentage point improvement over the suboptimal  $\mu = 0.1$  con-

figuration. The 4-client setup, whilst showing the same optimal  $\mu$  value, achieved  $79.0 \pm 3.22\%$  accuracy, indicating the trade-offs inherent in increased federation complexity.

**Sensitivity Analysis and Performance Degradation:** The results demonstrate FedProx’s considerable sensitivity to  $\mu$  selection, with performance varying substantially across the tested range. Higher  $\mu$  values ( $\mu = 1.0$  and above) consistently underperformed across all client configurations, with the 4-client,  $\mu = 1.0$  configuration achieving only  $74.8 \pm 2.79\%$  accuracy—the poorest performance observed. Conversely, intermediate values such as  $\mu = 0.1$  showed inconsistent behaviour, performing reasonably well with 2 clients ( $80.2 \pm 2.2\%$ ) but deteriorating significantly with increased client numbers. This pattern suggests that the proximal regularisation strength must be carefully calibrated to the federation’s complexity and statistical heterogeneity.

**Client Scaling Effects:** The interaction between client number and  $\mu$  sensitivity reveals important scalability considerations. The 3-client configuration demonstrated the most favourable performance profile, suggesting an optimal balance between federation complexity and coordination benefits. However, the 4-client setup showed increased variance and generally reduced performance across most  $\mu$  values, indicating that larger federations may require more sophisticated parameter tuning strategies. The consistent preference for very small  $\mu$  values ( $10^{-5}$ ) across all configurations suggests that minimal proximal regularisation provides sufficient coordination whilst preserving local adaptation capabilities.